

Performance Optimization of Bifacial Solar PV Modules Under Varied Albedo Conditions

Ryan Otieno Okoth

153038

Dissertation Submitted in Partial Fulfillment of the Requirements of the degree of Master of Science in Sustainable Energy Transitions

School of Computing and Engineering Sciences

Strathmore University

Nairobi, Kenya



This Dissertation is available for Library use through open access on the understanding that it is a copyright material and that no quotation from the Dissertation may be published without proper acknowledgement

Declaration and Approval

Declaration

I declare that this work has not been previously submitted and approved for the award of a degree by this or any other University. To the best of my knowledge and belief, the dissertation contains no material previously published or written by another person except where due reference is made in the dissertation itself.

© No part of this dissertation may be reproduced without the permission of the author and Strathmore University

Ryan Otieno Okoth



3rd June, 2025

Approval

The dissertation of Ryan Otieno Okoth was reviewed and approved by the following:

Dr. Allan Omondi

Lecturer, School of Computing and Engineering Sciences,
Strathmore University

Dr. Julius Butime

Dean, School of Computing and Engineering Sciences,
Strathmore University

Prof. Benard Shibwabo

Director of Graduate Studies,
Strathmore University



Abstract

This study addresses the knowledge gap concerning the performance optimization of bifacial solar photovoltaic (PV) modules under varying albedo conditions in Kenya. Albedo is a key factor influencing energy generation in solar applications. However, the extent of its impact in Kenya, particularly for bifacial modules, remains underexplored. With increasing interest in bifacial technology, understanding its operational efficiency in real-world scenarios is crucial, especially in tropical climates such as Kenya.

The study employed an experimental research method involving systematic measurements of albedo, irradiance, and module cell temperature across multiple setups of bifacial PV modules mounted at different heights. The aim was to assess the performance variation under different ground surface reflectivity conditions. Two distinct surface types were evaluated: concrete and grass. For each surface, five experiments were conducted using mounting heights of 0 m, 0.5 m, 1.0 m, 1.5 m, and 2.0 m. The results revealed that higher albedo surfaces significantly enhance energy output, with concrete surfaces consistently outperforming grass due to their higher reflectivity. For example, at a mounting height of 2.0 m, concrete surfaces achieved a maximum power output (P_{max}) of 432 W compared to 389 W on grass surfaces. Similarly, at ground level, concrete surfaces recorded 332 W, while grass surfaces yielded 325 W.

Furthermore, within the same surface type, energy output increased with greater mounting height. A case of this was an energy yield of 332 Watts at ground-level mounting and 389 Watts at 2m mounting height for grass surfaces. Similarly, ground-level mounting registered 325 Watts for concrete surfaces, while 2m height registered 432 Watts. On the same note, the study established that varying mounting height significantly increases rear-side irradiance; thus, the combination of albedo and mounting height can influence the performance of bifacial PV modules. Furthermore, the developed optimization model effectively predicts performance outcomes, highlighting the importance of tailored installation strategies. These findings suggest that optimizing the installation of bifacial solar systems can lead to significant energy efficiency improvements, thereby contributing valuable insights to renewable energy and promoting sustainable energy practices.

In conclusion, this study demonstrated that optimizing bifacial solar PV modules under varying albedo conditions significantly improves energy yield, especially with high-albedo surfaces like concrete and optimal mounting configurations. It recommends adopting bifacial modules with reflective surfaces, appropriate tilt angles, and mounting heights for maximum performance. Future research should focus on long-term performance data, advanced simulations, and broader environmental factors to refine predictive models and guide policy development.



Table of Contents

Declaration and Approval	ii
Abstract	iii
Table of Contents	v
List of Figures	viii
List of Tables	ix
List of Abbreviations & Acronyms	x
Definition of Key Terms	xi
Acknowledgement	xii
Chapter 1: Introduction	1
1.1 Study Background	1
1.2 Problem Statement	3
1.3 Study Objectives	3
1.3.1 Main Objective	3
1.3.2 Specific Objectives	3
1.4 Research Questions	3
1.5 Justification of the Study	4
1.6 Scope and Limitations of the Study	5
1.6.1 Study Limitations	5
Chapter 2: Literature Review	6
2.1 Introduction	6
2.2 Theoretical Literature Review.....	6
2.2.1 Photovoltaic (PV) Modules	6
2.2.2 Monofacial and Bifacial PV Module Technologies	11
2.2.3 Optimization of Bifacial Modules	16

2.3 Empirical Literature Review	19
2.3.1 Performance Comparison	20
2.3.2 Strategies for Optimizing Bifacial Modules	21
2.3.3 Albedo and Bifacial Performance.....	23
2.3.4 Gap Analysis of Empirical Literature Review on The Current Study.....	27
2.4 Conceptual Framework	28
Chapter 3: Methodology.....	30
3.1 Introduction	30
3.2 Research Method.....	30
3.3 Experimental Setup	30
3.3.1 Material and Equipment for Data Collection	31
3.3.2 Testing Procedure	33
3.4 Inclusion/Exclusion Criteria.....	35
3.5 Reliability and Validity of Research Instruments	35
3.5.1 Data Analysis.....	35
3.5.2 Modeling for Irradiance Reaching the Rear Surface.....	35
3.5.3 Data Preparation and Exploratory Data Analysis.....	36
3.5.4 Model Development	36
3.6 Ethics in Research	38
3.7 Dissemination of Results.....	38
3.8 Utilization of Research.....	39
Chapter 4: Results And Discussion	40
4.1 Introduction	40
4.2 Experimental setup.....	40
4.2.1 Bifacial Solar PV Module Setup on Concrete Surface.....	42

4.2.2 Solar System on Grass Surface.....	42
4.3 Data Presentation.....	43
4.3.1 Performance Output on Concrete Surface Setup.....	43
4.3.2 Performance Output on Grass Surface Setup.....	44
4.3.3 Solar PV module on Concrete and Grass Surfaces Power Output Comparison.....	46
4.3.4 Irradiance Comparison between Solar PV modules on Concrete and Grass Surface ..	47
4.3.5 Cell Temperature Comparison between PV Module on Concrete and Grass Surface .	48
4.3.6 Fill Factor Comparison between Solar PV Module on Concrete and Grass Surface ...	49
4.4 Model Development.....	49
4.4.1 Testing the Predictive Model.....	49
4.4.2 Developing Optimization Model.....	53
4.4.3 Testing the Optimization Model.....	56
4.5 Discussions of Findings	61
4.5.1 Impact of Albedo Conditions	61
CHAPTER FIVE CONCLUSION AND RECOMMENDATION.....	64
5.1 Conclusion.....	64
5.2 Recommendations	65
5.2.1 Practical Recommendations	65
5.2.2 Recommendations for Future Studies.....	65
References.....	67
Appendices.....	73
A- similarity Index	73
B – Ethical Clearance Approval.....	75
C – NACOSTI Research Certificate	76
D – PVA-1500 PV Analyzer Calibration Certificate	77

List of Figures

Figure 2.1: Solar cell, Solar module, and solar Array (Adam, 2019)	7
Figure 2.2: Single-Junction Back Contact Solar Structure (Source: Guerra et al., 2018)	8
Figure 2.3: A simple solar cell model.....	9
Figure 2.4: N-Type and P-Type Semiconductor.....	10
Figure 2.5: Illustration of Photovoltaic Effect	10
Figure 2.6: Monofacial and bifacial Source: (Kılıcı & Koklu, 2020).....	13
Figure 2.7: Working Of A Bifacial PV Module	14
Figure 2.8: Conceptual Framework	29
Figure 4.1: Mounting Stand Side view dimensions	40
Figure 4.2: Mounting stand adjustable Levels.....	41
Figure 4.3: Top view dimensions.....	41
Figure 4.4: 3D Illustration.....	41
Figure 4.5: Bifacial PV Module Mounted on a Concrete Surface.....	42
Figure 4.6: Bifacial PV Module Mounted on a Grass Surface	43
Figure 4.7: Concrete and Grass Surfaces Power Output Comparison	46
Figure 4.8: Irradiance Level Comparison Between Concrete and Grass Surface.....	47
Figure 4.9: Cell Temperature Comparisons Between Concrete and Grass Surfaces.....	48
Figure 4.10: Fill Factor (FF) Comparison Between Concrete and Grass Surface	49
Figure 4.11: Concrete Surface Predicted Output Measured Power Output	52
Figure 4.12: Grass Surface Predicted Output Measured Power Output	53
Figure 4.13: Excel's Solver Parameters Framework	55

List of Tables

Table 2.1: Summary of the albedo values for various surfaces	16
Table 2.2: Summary of Literature Review	25
Table 3.1: Data Sheet Recorded.....	31
Table 3.2: PV Module Details	32
Table 3.3: PVA-1500 PV Analyzer Model Characteristics	33
Table 4.1: Experiment Timelines for Concrete Surface Setup	42
Table 4.2: Experiment Timelines for Grass Surface Setup.....	43
Table 4.3: PV Module Performance Results by Height Level on Concrete Surface	44
Table 4.4: : PV Module Performance Results by Height Level on Grass Surface	44
Table 4.5: Performance Optimization Formula Test for Different Surfaces and Mounting Height Levels	52
Table 4.6: Optimum Albedo, Mounting Height, and Tilt Angle Derived from Solar PV module on a Concrete Surface Measured Parameters.....	57
Table 4.7: Optimization Model Test for Solar PV module on Concrete Surface (Absolute Albedo value).....	58
Table 4.8: Optimum Albedo, Mounting Height, and Tilt Angle Derived from Solar PV Module on a Grass Surface Measured Parameter	59
Table 4.9 Optimization Model Test for Solar PV Module on Grass surface (Absolute Albedo value).....	60

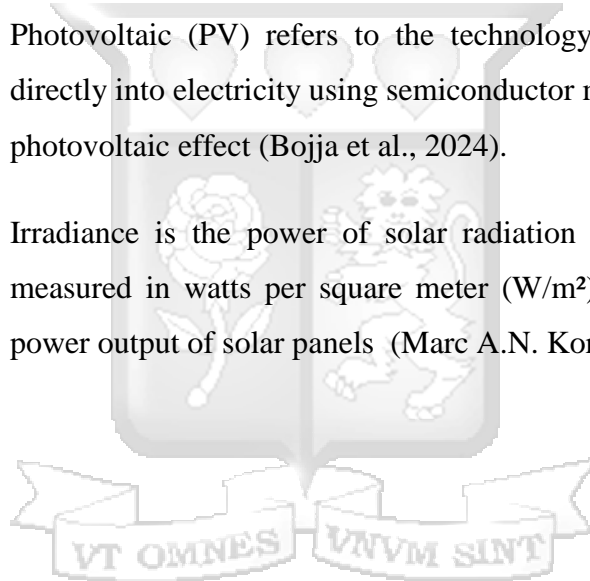
List of Abbreviations & Acronyms

AL-BSFC	Aluminium Back Surface Field Cells
EQE	External Quantum Efficiency
FF	Fill Factor
IEEE	Institute of Electrical and Electronic Engineers
PERC	Passivated Emitter Rear Cell
PERT	Passivated Emitter Rear Totally Diffused
PV	Photovoltaic
PVA	Photovoltaic Analyzer



Definition of Key Terms

Albedo	Albedo refers to the reflectivity of a surface, i.e., the fraction of solar radiation reflected from the ground back to the atmosphere (Schoenau et al., 2018.)
Bifacial PV Module	A bifacial PV module is a solar panel that can capture sunlight on both its front and rear sides, improving energy yield by utilizing reflected light from the ground or surroundings (Riedel-Lyngskær, Kopecek, Libal, & Urrejola, 2022).
Photovoltaic (PV)	Photovoltaic (PV) refers to the technology that converts sunlight directly into electricity using semiconductor materials that exhibit the photovoltaic effect (Bojja et al., 2024).
Irradiance	Irradiance is the power of solar radiation received per unit area, measured in watts per square meter (W/m^2). It directly affects the power output of solar panels (Marc A.N. Korevaar, 2022).



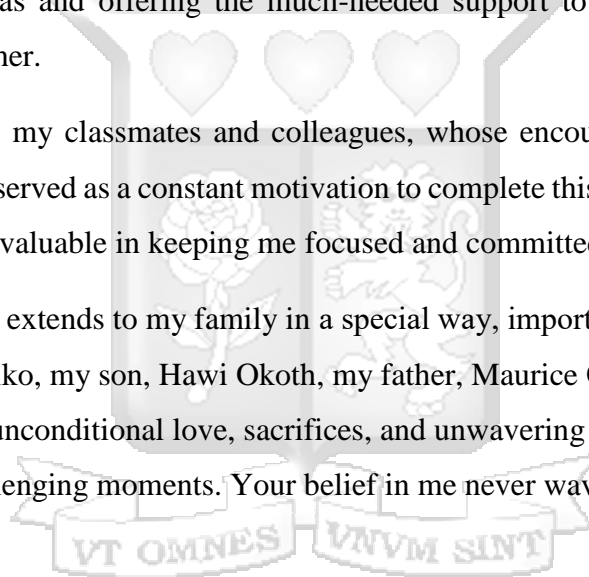
Acknowledgement

The writing of this dissertation has been a transformative journey of intellectual discovery, personal growth and unwavering support from remarkable individuals who have shaped my academic pursuits and personal resilience.

First and foremost, I want to extend my deepest gratitude to my supervisor Dr. Allan Omondi for his dedication and efforts to ensure I have grasped the necessary knowledge of research methodology. I cannot voice enough the dedication he has given me and all the opportunities to hone my practical skills in this area. Our interactions have achieved nothing short of gaining great insight into scientific research and academic writing. I thank Dr.Eng Fenwicks Musonye for his time listening to my ideas and offering the much-needed support to build confidence toward becoming a good researcher.

I am equally indebted to my classmates and colleagues, whose encouragement and reminders, though at times daunting served as a constant motivation to complete this work in a timely manner. Their support has been invaluable in keeping me focused and committed to my research.

My heartfelt appreciation extends to my family in a special way, importantly I'd like to mention - my wife, Stacey Nyandiko, my son, Hawi Okoth, my father, Maurice Okoth, my mother, Elector Achieng, whose unconditional love, sacrifices, and unwavering support have been my bedrock through the challenging moments. Your belief in me never wavered



Chapter 1: Introduction

1.1 Study Background

As the world's population grows, along with technological advancements and climate change, so does the demand for clean and reliable energy. Conventional energy sources such as fossil fuels have been deemed finite and major contributors to greenhouse gas emissions and climate change. There has been a pressing issue of transitioning to more sustainable and environmentally friendly energy solutions. Solar Photovoltaic (PV) is a widely used technology that harnesses the Sun's energy to create electricity, reducing reliance on traditional non-renewable energy sources.

The introduction of bifacial solar PV modules represents a significant advancement in photovoltaic technology, holding considerable promise for improving energy generation efficiency (Bojja et al., 2024). Unlike traditional monofacial modules that capture sunlight from only one side, bifacial modules are designed to absorb light from both their front and rear surfaces. This dual-sided capability allows them to utilize not only direct sunlight but also reflected light (albedo) from the ground or surrounding surfaces, thereby increasing their overall energy yield and potentially leading to higher power output per unit area (Schoenau et al., 2018).

Therefore, albedo conditions can be strategically exploited to significantly improve the design efficiency of bifacial modules. By carefully considering the reflective properties of the surface beneath the modules, such as light-colored gravel or white membranes, the amount of light reflected to the rear side of the bifacial modules can be maximized. However, despite this clear potential, there is currently a notable lack of published literature and comprehensive research specifically detailing the effects of varied albedo conditions on bifacial module performance. Much more study is required to fully understand and quantify this effect, enabling optimized design and deployment strategies for bifacial solar PV systems.

Bojja et al. (2024) explain that the bifacial solar PV systems technology was introduced as a promising solution to the increasing demand for renewable energy. This solution comes from this technology's capacity to deliver higher energy output while occupying less space than monofacial PV systems. The author further asserts that this technology does more than address rising energy demands, including lowering operating costs and carbon emissions, which aligns with sustainability goals. The bifacial solar PV modules have been adopted because of their efficiency

which comes from first, the dual sided nature that allows it to capture sunlight from both rear and front side by taking advantage of the reflect light.

The introduction of bifacial solar PV modules represents a significant advancement in photovoltaic technology, holding considerable promise for improving energy generation efficiency. Unlike traditional monofacial modules that capture sunlight from only one side, bifacial modules are designed to absorb light from both their front and rear surfaces. This dual-sided capability allows them to utilize not only direct sunlight but also reflected light (albedo) from the ground or surrounding surfaces, thereby increasing their overall energy yield and potentially leading to higher power output per unit area.

Therefore, drawing from albedo's contribution to enhancing these solar PV modules efficiency, there is an implication that such albedo conditions can be leveraged in designing efficiency of these bifacial modules. Nonetheless, there is still very limited scholarly investigation of this effect on bifacial modules. Despite the clear potential of albedo conditions to significantly enhance the design efficiency of bifacial modules, there remains a notable scarcity of published literature and research specifically exploring this phenomenon. Extensive further study is critically required to fully understand and quantify the impact of varied albedo conditions on bifacial PV module performance, which in turn can inform optimized module design and deployment strategies.

Photovoltaic (PV) modules convert solar energy into electricity using solar cells, with monofacial and bifacial modules being the two main types. Monofacial PV modules are the conventional technology that absorbs sunlight from only one side and are limited by environmental factors such as irradiance and albedo. In contrast, bifacial PV modules represent a technological improvement, capturing solar irradiance on both the front and rear surfaces, thereby increasing efficiency. The performance of bifacial modules is significantly influenced by factors such as ground reflectivity (albedo), mounting configuration, and installation conditions, offering potential energy gains particularly in high-albedo environments such as snowy or sandy areas (Riedel-Lyngskær, Kopecek, Libal, & Urrejola, 2022).

1.2 Problem Statement

Bifacial solar PV modules, engineered to capture sunlight through both the rear and front surfaces, have emerged as a potential enhancement to conventional PV technology. These modules promise increased energy production by utilizing reflected sunlight from the ground surface albedo, particularly in environments characterized by high surface reflectivity such as snow-covered terrains, arid desert regions, and areas with naturally light-colored soils.

Despite the growing interest in bifacial PV technology, there is a significant gap in understanding how these modules perform in solar systems across various albedo conditions. While theoretical studies suggest potential benefits, empirical evidence and systematic evaluations of their performance in practical applications remain limited. This research addresses this knowledge gap by comprehensively assessing the performance of bifacial solar PV modules under varied albedo conditions.

1.3 Study Objectives

1.3.1 Main Objective

The main objective of this study is to optimize the performance of solar PV systems using bifacial PV modules under varied albedo conditions, with a focus on tropical environments.

1.3.2 Specific Objectives

- i. To evaluate the impact of tropical albedo conditions on the performance of bifacial PV modules.
- ii. To analyze the design attributes such as installation height and row spacing for enhanced performance of bifacial PV modules.
- iii. To design an optimization model that can effectively predict and optimize the performance of bifacial solar PV modules under varying tropical albedo conditions in Kenya.
- iv. To validate the developed optimization model using empirical data and simulations

1.4 Research Questions

- i. How do tropical albedo conditions affect the performance of bifacial PV modules?
- ii. How can design attributes such as installation height and row spacing be estimated or optimized to improve the performance of bifacial PV modules?

- iii. How can an optimization model be developed to predict and enhance the performance of bifacial solar PV modules under varied tropical albedo conditions in Kenya?
- iv. How can the accuracy and reliability of the developed optimization model be validated using empirical data and simulations?

1.5 Justification of the Study

Accessing reliable, affordable, and clean energy is crucial to socioeconomic development and achieving the Sustainable Development Goals (SDG), which aim to ensure universal access to cheap, reliable, and sustainable energy by 2030. Like the rest of the developing nations, Kenya has consistent energy challenges, including inadequate access to electricity in rural areas, depending on fossil fuels, and the increasing pressure to diversify renewable energy sources.

This study recognizes that solar PV technology has been identified as a promising solution for sustainable energy generation. Nonetheless, the effectiveness and efficiency of this technology are influenced by various environmental and design factors. Focusing on the Kenyan context, there are unique albedo conditions due to the varying surfaces, vegetation, and climatic patterns. These conditions present both opportunities and challenges regarding optimizing the performance of bifacial solar PV modules.

Additionally, social and economic challenges, such as energy poverty, economic disparity, and limited access to renewable energy technologies, assert the urgency for advancing innovative solutions to enhance solar PV performance and deployment. By addressing these challenges, this study aligns with global efforts to improve energy access and support initiatives like the SDG& and Kenya's Vision 2030, whose priorities include renewable energy development. Lastly, the study contributes to the objective of the Better Energy Transition Access (BETA) initiative by demonstrating how optimized bifacial PV modules can provide cost-effective and sustainable energy solutions in tropical regions.

Designing the optimization model that tailors the Kenyan-specific albedo and environmental conditions is vital in advancing local renewable energy strategies, reducing dependency on nonrenewable sources, and promoting energy equity.

1.6 Scope and Limitations of the Study

This study assessed the performance of bifacial solar PV modules under varied albedo conditions, with a focus on tropical environments. It examined how surface reflectivity influences the energy output of bifacial modules by comparing their performance against monofacial modules under controlled conditions. However, the study was limited to selected tropical scenarios, and the results may not be directly transferable to other climatic regions. Additionally, the use of controlled albedo settings may not fully replicate the variability found in real-world conditions, and the availability of high-resolution empirical data posed constraints on the accuracy of model validation.

1.6.1 Study Limitations

- i. The research was conducted in a controlled environment with limited albedo variation, which does not fully reflect the range of conditions typically encountered in real-world deployments that experience more diverse environmental influences.
- ii. The study did not capture long-term performance trends due to the limited timeframe allocated for data collection; as a result, long-term performance outcomes remain speculative and outside the scope of this research.
- iii. The use of a specific solar PV module configuration and test location limits the generalizability of the findings. Broader applicability would require further research involving diverse system designs and geographical contexts.

This research addressed the identified limitations by acknowledging their existence and discussing potential methods for future research to address them. These include long-term monitoring or wider field testing across diverse locations. Furthermore, the study chose data collection methodologies that ensure robust and reliable results within the defined research scope.

This research will address the identified limitations by acknowledging their existence and discussing potential methods for future research to address them. These include long-term monitoring or wider field testing across diverse locations.

Chapter 2: Literature Review

2.1 Introduction

This chapter provides a comprehensive review of both theoretical and empirical literature relevant to the optimization of bifacial photovoltaic (PV) modules under varying environmental conditions. It begins by outlining the fundamental principles of photovoltaic technology and progresses to discuss the differences between monofacial and bifacial modules, emphasizing their structural and performance characteristics. Furthermore, it explores optimization strategies for bifacial modules, focusing on critical parameters such as albedo, tilt angle, and mounting height. The chapter also integrates empirical findings from existing studies, identifying gaps and establishing the contextual relevance of this study within the Kenyan setting. Overall, this literature review aims to build a strong foundation for understanding how environmental and design factors influence bifacial PV performance, informing the development of an effective optimization model.

2.2 Theoretical Literature Review

2.2.1 Photovoltaic (PV) Modules

In a solar photovoltaic (PV) module, the most essential component is the solar cell—a device that converts light energy into electrical energy through the photovoltaic effect. A single solar cell produces only a small amount of electricity, typically sufficient for powering low-energy devices such as calculators or small light bulbs (Solar Energy Technologies Office, 2022). To increase energy output, multiple solar cells are connected and embedded between protective materials, typically two glass sheets, to form a solar module. Interconnecting multiple modules results in a solar array, which provides a larger surface area for sunlight absorption and significantly greater power generation. Figure 2.3 illustrates these differences.

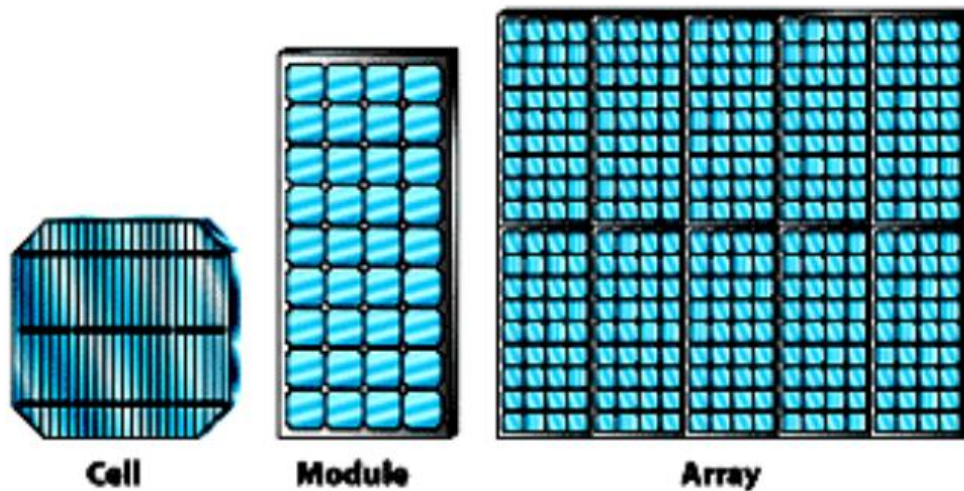


Figure 2.1: Solar cell, Solar module, and solar Array (Adam, 2019)

The first frame represents the solar cell which is also the smallest component in a solar PV system. Several solar cells make a complete module, as shown in the second frame. In a typical solar PV plant, several modules are interconnected to form the array as presented in the third frame.

2.2.1.1 Operating Principles of a Solar Cell

The operating principle of a silicon solar cell is based on the photovoltaic effect, a phenomenon discovered in 1839 by French physicist Alexandre Edmond Becquerel. The photovoltaic effect refers to the process by which photons of light excite electrons within a material, resulting in the formation of electron-hole pairs. When these electrons gain enough energy to move from the valence band to the conduction band, an electric current is generated. According to Guerra et al. (2018), this effect is closely related to the photoelectric effect later described by Albert Einstein in 1905.

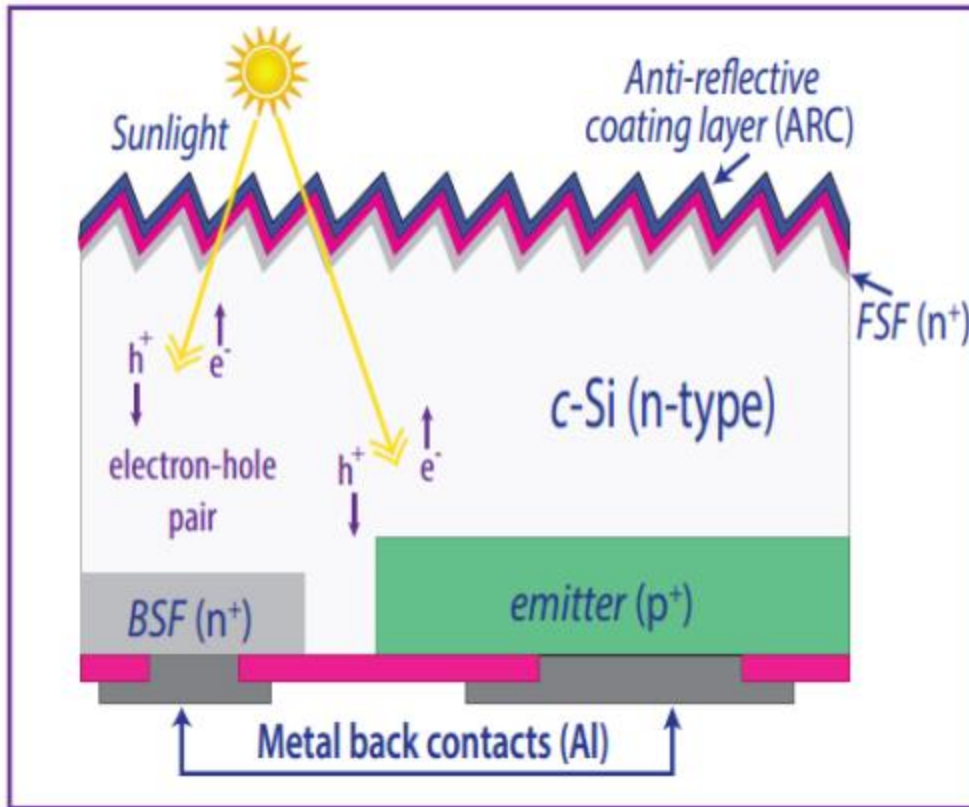


Figure 2.2: Single-Junction Back Contact Solar Structure (Source: Guerra et al., 2018)

The PV effects occur in 3 steps:

- i. Generation of charge carriers: When sunlight strikes the surface of the semiconductor material, photons are absorbed by the material, transferring their energy to electrons. This energy excites the electrons, allowing them to break free from their atomic bonds and generate electron-hole pairs. Some photons may be reflected or transmitted, but those with sufficient energy are absorbed, initiating the photo-generation process (Guerra et al., 2018).
- ii. Separation of charge carriers: The internal electric field created by the p-n junction drives the separation of the photo-generated electron-hole pairs. Electrons are directed toward the n-type side, while holes move toward the p-type side. This separation prevents recombination and sets up the potential for electrical current (Guerra et al., 2018).
- iii. Collection of charge carriers and current generation: The separated charge carriers are collected by metal contacts on the cell's surface, allowing them to flow through an external circuit. As electrons move through the load, electrical energy is delivered to the external

circuit. Eventually, the electrons recombine with holes on the opposite side of the device, typically at a metal contact surface (Guerra et al., 2018).

Figure 2.3 summarizes these three steps.

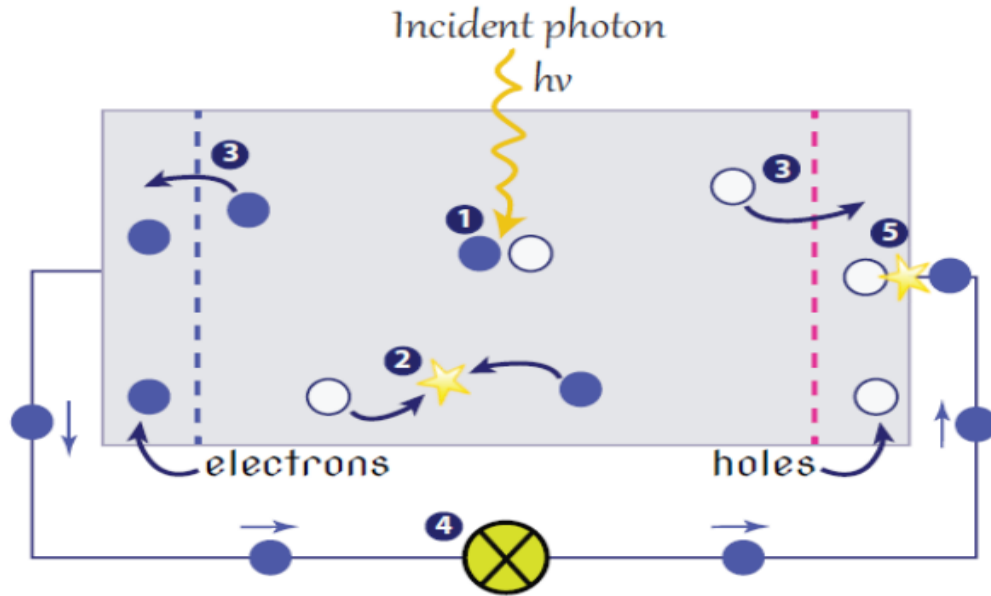


Figure 2.3: A simple solar cell model

(Guerra et al., 2018)

As illustrated in Figure 2.3, the photovoltaic (PV) effect unfolds through several distinct stages. Point 1 indicates the region where incoming photons are absorbed by the semiconductor material, resulting in the generation of electron-hole pairs. Point 2 marks the initial presence of both electrons and holes before they are separated. Point 3 shows the action of the internal electric field at the p-n junction, which drives the separation of electrons toward the n-type material and holes toward the p-type material. At Point 4, the separated electrons flow through an external circuit, generating electric current. Finally, Point 5 depicts the electrons reuniting with holes at the back contact, completing the circuit. These stages collectively demonstrate the conversion of light energy into usable electrical energy via the photovoltaic effect (Guerra et al., 2018).

2.2.1.2 Materials used in Solar Cells

According to Adam (2019), 95% of solar cells produced globally use the semiconductor material Silicon (Si). This is also the second most abundant element on the Earth's crust; therefore, it is

available in more than enough quantities. The solar cell is produced by contaminating the semiconductor, also called doping. A dope semiconductor is one in which chemical elements have been intentionally introduced. Adam (2019) further explains that the doping process depends on the dopant type: a surplus of positive charge carriers (the p-conducting semiconductor layer) or negative charge carriers (the N-conducting semiconductor layer).

p-n junction is formed on the boundary layers when two differently contaminated semiconductor layers are combined. This is illustrated in Figure 2.4

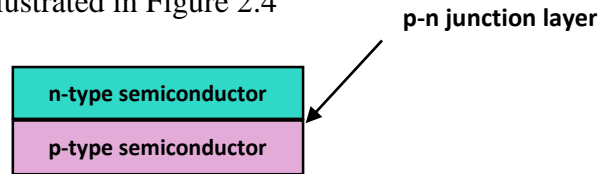


Figure 2.4: N-Type and P-Type Semiconductor

source: (Adam, 2019)

The p-type semiconductor (with excess holes) is obtained when a trivalent element is doped. In contrast, an n-type semiconductor (with excess electrons) is obtained when a pentavalent element is doped.

2.2.1.3 Electron Hole

According to Adam (2019), a clear day has about 4.4×10^{17} photons strike per square centimeter of the Earth's surface per second. Of this energy, only the photons with energy over the band gap can be converted into electricity by the solar cell. When this photon enters the semiconductor, it can be absorbed and promote an electron from the valence band to the conduction band, as illustrated by Figure 2.5

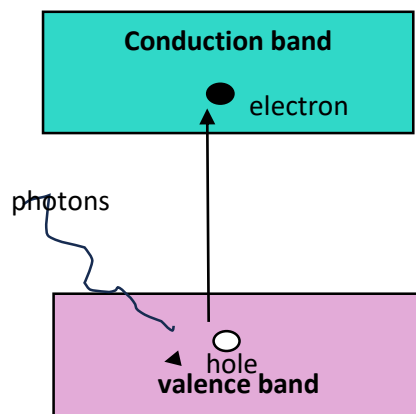


Figure 2.5: Illustration of Photovoltaic Effect

Source: (Adam, 2019)

A hole is created when an electron is promoted, creating a vacant hole (hence the hole). At this stage, the electron in the conduction band and the hole in the valence band combine to form electron-hole pairs. This is also the primary mechanism within a single solar cell. The most commonly known solar cell is configured as a large p-n junction made from a silicon wafer (Adam, 2019).

2.2.1.4 N-type vs. P-type

While both P-type and N-type technologies constitute the pillar of the solar industry by working to convert sunlight into electricity beneath the surface, they have subtle differences that influence their performance. The basic difference between the two technologies lies in the doping method. In p-type technologies, boron atoms with one less electron than silicon are introduced, creating a positive charge carrier (hole) majority. In n-type technologies, phosphorous atoms with one extra electron are introduced to create a negative charge carrier (electron) majority.

N-type and P-type technologies work effectively; however, the N-type cells exhibit distinct advantages. For instance, they have superior efficiency as they have less light-induced degradation (LID) over time. On the other hand, p-type cells tend to decline in performance due to the interaction between oxygen and boron. This follows that the main reason why N-type cells have higher long-term output compared to p-type cells is due to their lower degradation (Adam, 2019).

N-type cells also exhibit better temperature coefficients compared to p-type cells. The latter tend to experience a significant drop in efficiency when subjected to a higher temperature. Ultimately, the n-type cells are better suited for hot and sunny climates.

Nonetheless, P-type cells remain widely used since they have established manufacturing, which is cost-effective, making them more affordable. Something important to take into consideration is that historically, the p-type cells have been the more commonly used of the two, giving them a sense of reliability and familiarity (Jäger-Waldau, 2020).

2.2.2 Monofacial and Bifacial PV Module Technologies

Photovoltaic (PV) modules are categorized primarily into monofacial and bifacial technologies based on the direction(s) from which they absorb sunlight. Although both types rely on the photovoltaic effect to convert solar energy into direct current (DC) electricity, their architectural

designs differ significantly. This distinction greatly influences their efficiency, installation strategies, and performance under varying environmental conditions.

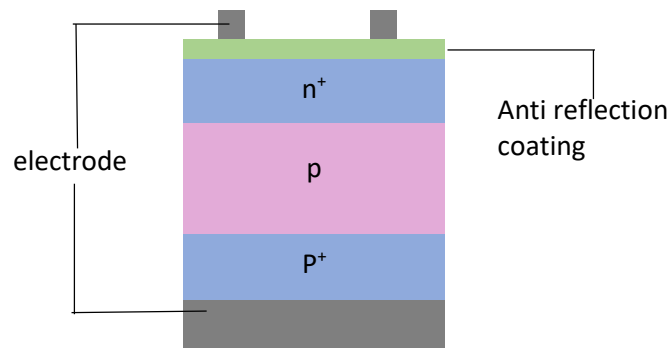
2.2.2.1 Monofacial PV Modules

Monofacial PV modules represent the conventional and most widely deployed solar panel technology. These modules are built with solar cells that absorb light exclusively from the front surface, rendering the rear side inactive. Typically, monofacial cells are manufactured using p-type silicon wafers combined with an aluminum back surface field (Al-BSF) layer that serves as a rear electrical contact while also being completely opaque to light (Raina & Sinha, 2020). As a result, any reflected sunlight from the ground—referred to as albedo—is not utilized, thereby limiting energy yield to direct and diffuse irradiance from the sky.

One of the defining advantages of monofacial modules is their low manufacturing cost. The long-established industrial processes for fabricating p-type cells contribute to their affordability and market dominance (Renato, 2015). Moreover, their mechanical simplicity and compatibility with traditional mounting systems make them well-suited for both small-scale residential systems and large-scale utility installations (Gevorkov, Domínguez-García, & Romero, 2022). Another often-cited strength is their proven reliability, which is based on decades of field deployment under diverse climatic conditions.

However, monofacial modules do face performance limitations. Their energy production is directly tied to the amount of sunlight striking the front surface, which fluctuates throughout the day and across seasons. Overcast weather, shadows, or lower sun angles during winter months reduce irradiance and can notably impact output. Furthermore, these modules do not benefit from the ground's reflectivity, making them suboptimal in environments with high-albedo surfaces such as snow-covered fields or desert sand (Renato, 2015). This is illustrated in Figure 2.6, where the opaque back layer blocks all rear-side irradiance from contributing to energy generation.

Monofacial solar cell



bifacial solar cell

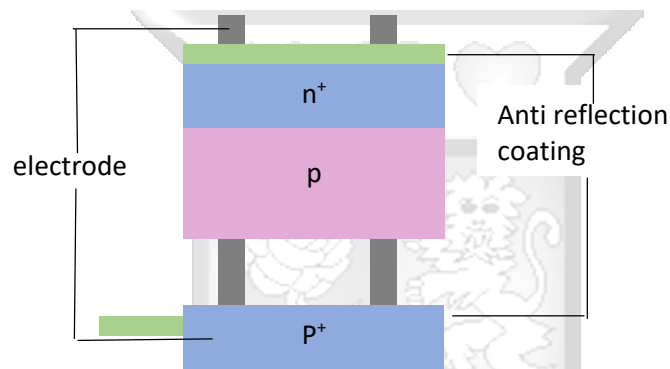


Figure 2.6: Monofacial and bifacial Source: (Kılıcı & Koklu, 2020)

Despite these drawbacks, the simplicity, economic feasibility, and extensive performance history of monofacial PV systems have made them a default choice for many solar projects worldwide.

2.2.2.2 Bifacial PV Modules

Bifacial PV modules, on the other hand, are a more technologically advanced alternative that allows light to be absorbed from both the front and rear surfaces of the module. This dual-sided configuration is enabled by advanced cell architectures such as Passivated Emitter Rear Cell (PERC), Passivated Emitter and Rear Totally Diffused (PERT), and Heterojunction with Intrinsic Thin layer (HIT) cells (International Energy Agency, 2021). These designs incorporate transparent or semi-transparent back contacts that permit light to enter the rear side, enabling the absorption of ground-reflected irradiance.

A critical structural distinction of bifacial cells is that they may utilize either p-type or n-type silicon substrates, though n-type silicon is often preferred in high-performance modules. N-type wafers are inherently less susceptible to light-induced degradation (LID) and maintain performance stability over time, especially in high-temperature or high-irradiance environments (Kılıcı & Koklu, 2020). Additionally, n-type cells exhibit higher carrier lifetimes and temperature tolerance, giving them an edge in terms of efficiency and durability over traditional p-type counterparts.

In Figure 2.7, the basic working principle of a bifacial solar module is visualized. When sunlight strikes the front of the module, direct irradiance is converted to electricity in the usual manner. Simultaneously, ground-reflected sunlight—known as albedo—is allowed to pass through the back surface via finger grids or transparent layers, contributing additional electron-hole pair generation.

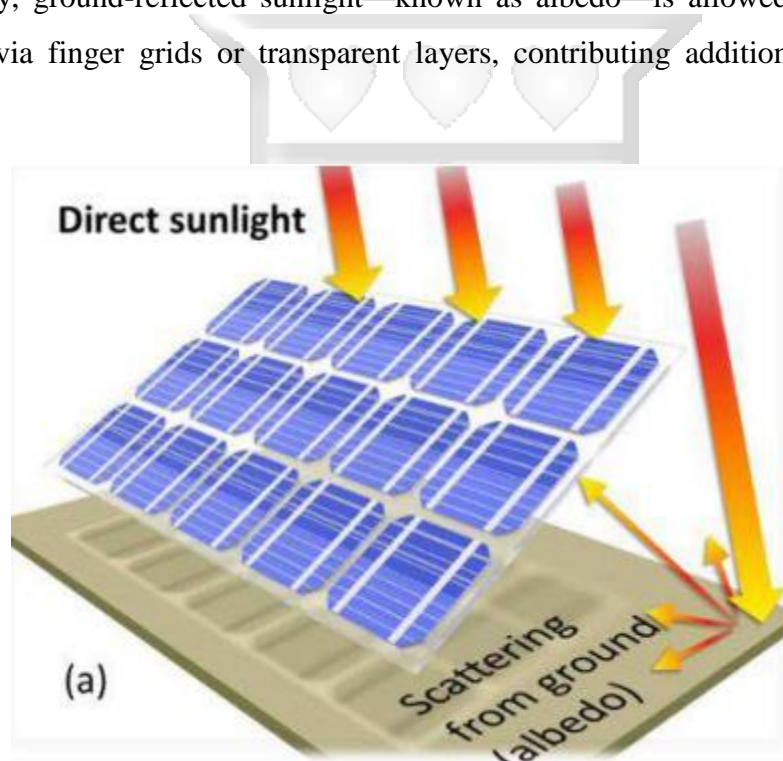


Figure 2.7: Working Of A Bifacial PV Module

Source: (Osama Ayadi et al., 2021)

An important metric associated with bifacial solar PV modules is the bifaciality factor, which is defined as the ratio of power produced by the rear side to that generated by the front side under identical conditions. This factor typically ranges between 70% and 95% (Shishavan, 2019). A

bifaciality factor of 80%, for instance, indicates that the rear surface can contribute up to 80% of the energy that the front side produces under standard test conditions.

The energy gain provided by bifacial modules is heavily influenced by site-specific conditions. One of the most significant of these is albedo. High-albedo surfaces such as snow (albedo ≈ 0.8), white gravel, or sandy deserts can significantly enhance rear-side irradiance, boosting overall module efficiency by 10–20% compared to monofacial modules (Ganesan, 2023; Riedel-Lyngskær et al., 2022). As detailed in Figure 2.6, the structural differences between monofacial and bifacial modules reveal how bifacial designs optimize light absorption via rear-side exposure.

Beyond albedo, factors such as module elevation, row spacing, mounting orientation, and tracker configuration can dramatically affect bifacial performance. For example, increased height allows more reflected light to reach the rear surface, while appropriate spacing reduces self-shading. Tracker systems, particularly dual-axis trackers, further optimize the angular alignment of the modules, maximizing exposure throughout the day.

Despite their higher initial cost due to the need for enhanced materials and complex manufacturing, bifacial modules often result in lower levelized cost of electricity (LCOE) over the system's lifetime when deployed in optimal conditions. Their long-term energy yield, especially in reflective environments, makes them a compelling solution for high-performance solar farms and utility-scale applications.

2.2.2.3 Comparative Analysis of Monofacial and Bifacial Modules

While both monofacial and bifacial PV modules are rooted in the same photovoltaic principles, their operational dynamics and environmental adaptability differ markedly. Monofacial modules are cost-effective and ideal for general-purpose installations with limited rear irradiance. Their opaque backsheets, simplified installation, and standardized supply chain make them ideal for urban rooftops, carports, and installations with low ground reflectivity.

In contrast, bifacial modules offer superior performance when paired with thoughtful system design in environments that maximize ground reflectance. Their dual-sided light absorption, higher efficiency, and reduced degradation under high-irradiance conditions make them well-suited for snow-prone regions, deserts, and systems with reflective surfaces or elevated mounting.

As outlined in Table 2.1, bifacial modules require more advanced engineering strategies to achieve their potential gains. When optimized, however, they can significantly outperform their monofacial counterparts, particularly in utility-scale deployments focused on maximizing annual yield and minimizing degradation losses.

Table 2.1: Summary of the albedo values for various surfaces

Surface	Albedo
Aluminum	0.85
Fresh Snow	0.82
Copper	0.74
Wet snow	0.55-0.75
New Galvanized steel	0.35
Concrete	0.25-0.35
Red tiles	0.33
Fresh grass	0.26
Grass	0.15-0.25
Urban environment	0.14-0.22
Wet Asphalt	0.18
Dry asphalt	0.09-0.15
Very Dirty Galvanized	0.08

Source: (PVsyst Help Contents, 2024)

2.2.3 Optimization of Bifacial Modules

The deployment of bifacial photovoltaic PV modules introduces a range of engineering considerations that go beyond those associated with monofacial PV modules. While both types are installed using similar structural methods, the optimization of bifacial systems is significantly more complex due to their ability to generate electricity from both the front and rear surfaces. This dual-surface generation is influenced by several variables, including albedo, backside shading, irradiance mismatches, and electrical stringing design. Maximizing the performance of bifacial systems, therefore, requires a deeper understanding of these unique challenges.

2.2.3.1 Albedo (Ground Reflectance)

One of the most critical factors affecting the efficiency of bifacial modules is albedo, which is defined as the fraction of solar radiation reflected from the ground surface back toward the module's rear side. Surfaces with high reflectivity, such as fresh snow or aluminum, can significantly enhance the rear-side irradiance and thereby improve energy output. For example,

fresh snow can exhibit an albedo value between 0.82 and 0.90, while aluminum surfaces can reach up to 0.85 (PVsyst Help Contents, 2024; Alexander et al., 2014). In contrast, darker and less reflective surfaces such as dry asphalt may have an albedo as low as 0.09.

The reflective properties of the ground can vary significantly depending on location, surface type, season, and weather conditions. Consequently, the optimization of bifacial PV modules begins with an accurate assessment of site-specific albedo values, ideally measured monthly or seasonally to capture variations over time (Han & Kim, 2024). Bifacial systems perform exceptionally well in snowy regions or desert environments with naturally reflective surfaces. Additionally, developers sometimes enhance ground reflectivity by installing bifacial modules over artificially reflective materials such as white gravel or specially coated membranes to maximize rear irradiance (Sanjuán, Morales, & Zaragoza, 2021; Ganesan, 2023).

Moreover, performance gains can be further influenced by the mounting height of the module above the ground. Increasing the elevation generally improves the view factor—the proportion of the ground visible from the rear side of the panel—thus increasing the amount of reflected light captured. The higher the module from the ground, the larger the area from which it can receive reflected irradiance, although this also increases construction complexity and cost.

2.2.3.2 Backside Shading

While front-side shading is widely addressed during the design of both monofacial and bifacial systems, rear-side shading remains a particular concern for bifacial modules. Shading elements such as tracker posts, torque tubes, support structures, wiring trays, and combiner boxes can obstruct reflected light and significantly reduce rear-side energy gain (Pelaez, 2019). Unlike monofacial modules, where rear-side light is irrelevant, bifacial modules must account for obstructions behind the panels that may block reflected sunlight.

Reducing these sources of shade requires careful attention to tracker design and installation parameters. For instance, orienting torque tubes to minimize their projection onto the rear side or using smaller-diameter posts can increase exposure to reflected light. Likewise, increasing the row spacing and elevating the panels can reduce the likelihood of components casting shadows on the rear surface. While these adjustments may seem minor, their cumulative impact can significantly influence energy output, particularly in high-albedo environments.

2.2.3.3 Module Mismatch and Irradiance Nonuniformity

Another crucial factor in bifacial optimization is the mitigation of irradiance mismatch between modules, particularly across the rear side. Unlike the front surface, which typically receives relatively uniform sunlight, the rear surface is affected by localized variations in reflectivity, terrain, and shading. These variations can cause some modules to receive more rear-side irradiance than others, resulting in a mismatch when modules are connected in series (Kirsh, 2020).

When modules with different energy outputs are connected in the same string, the performance of the entire string is limited by the lowest-performing module. Over time, additional sources of mismatch such as light- and elevated temperature-induced degradation (LeTID), potential-induced degradation (PID), and encapsulant yellowing can exacerbate these disparities. To address this, system designers often employ module-level power electronics—such as optimizers or microinverters—to allow each module to operate independently at its maximum power point. Alternatively, grouping modules with similar rear-side exposure into the same string can also help minimize mismatch-related losses.

Accurate site modeling using irradiance simulation tools during the design phase can further aid in predicting and correcting potential mismatches before installation. Such tools can simulate different configurations, allowing for optimized string layouts that minimize performance disparities due to uneven rear-side irradiance.

2.2.3.4 Electrical Stringing and Layout Optimization

Electrical stringing in bifacial systems requires special attention due to potential differences in irradiance across rows. For instance, in tracker systems where two modules are mounted vertically (2P configuration), modules closer to the ground tend to receive less reflected light than those mounted higher. If modules from both rows are wired into the same string, this can create current mismatch, reducing the string's overall efficiency (Kirsh, 2020).

Similar challenges arise when comparing landscape and portrait module orientations. If rear-side irradiance is nonuniform across the horizontal or vertical axis and this pattern does not align with the internal cell string layout or bypass diodes, the efficiency losses can be substantial. To mitigate

this, module orientation must be chosen carefully based on site-specific irradiance patterns and structural design.

Additionally, designers must consider how elevation and string configuration influence the uniformity of irradiance. Grouping modules with similar rear-side exposure into dedicated strings can reduce mismatch. Parallel string configurations may also help isolate underperforming modules rather than having them degrade the performance of an entire series string.

2.2.3.5 Integration with Solar Trackers

The integration of bifacial modules with solar trackers is another essential strategy for maximizing energy yield. Trackers allow the modules to follow the Sun's path throughout the day, maintaining optimal orientation for front-side irradiance. In bifacial systems, this tracking also affects the angle and intensity of rear-side irradiance. Horizontal single-axis trackers (HSATs) are the most common and can enhance bifacial energy gains by 15–25% compared to fixed-tilt configurations (Urrejola et al., 2020).

To optimize performance, tracker systems must be designed to account for the bifacial-specific dynamics of light reflection and rear-side exposure. This includes adjusting the ground clearance and tilt angles to maximize both front and rear irradiance, as well as incorporating advanced tracking algorithms that consider the contribution of reflected light in addition to direct sunlight.

Thus, optimizing bifacial PV modules involves a multifaceted approach that incorporates environmental assessment, structural configuration, electrical design, and advanced tracking strategies. Each factor—albedo, backside shading, mismatch loss, electrical stringing, and tracker alignment—must be carefully engineered to ensure that the full potential of bifacial technology is realized. By addressing these variables holistically, bifacial systems can achieve significant performance advantages over traditional monofacial systems, ultimately offering a lower levelized cost of electricity and higher long-term energy yields.

2.3 Empirical Literature Review

In terms of scholarly exploration, the concept of performance of bifacial PV modules is a relatively new area. Most existing studies take the modeling and simulation methodological approaches, with very few based on actual measurements and testing methodological approaches. Besides, most of

these studies are based in the temperate region, presenting a colossal gap for tropical areas like Kenya. Nonetheless, these studies establish a fundamental framework and insights that can be used to guide the potential of this solar technology in, say, the Kenyan context. This empirical analysis categorizes the studies into three thematical focuses: performance comparison, optimization of bifacial modules, and albedo and bifacial performance.

2.3.1 Performance Comparison

A number of empirical studies have sought to compare the performance of bifacial PV modules to their monofacial counterparts under different environmental and operational conditions. Recent work by Guo et al. (2020) is particularly insightful in this regard. Their field measurements, conducted in a subtropical climate in southern China, analyzed both monofacial and bifacial module performance over a one-year period. The results showed that bifacial modules yielded approximately 11–14% more energy annually than monofacial modules when installed in elevated configurations over reflective surfaces such as light-colored gravel. The study further highlighted that the actual gain varied seasonally and was more pronounced during months with high solar angles and lower cloud cover. In another study by Asgharzadeh et al. (2019), empirical data was collected from a bifacial PV testbed in Albuquerque, New Mexico—a region with high solar irradiance. Their year-long evaluation confirmed that bifacial modules provided consistent performance gains, especially when paired with single-axis trackers. The energy gain was reported at around 13–20% compared to fixed-tilt monofacial systems. Interestingly, the authors noted that bifacial gains were not only dependent on albedo but also on other site-specific factors such as shading geometry, module elevation, and azimuth tracking precision.

A more recent study by Sun et al. (2023) carried out in Singapore—a tropical environment more akin to Kenya—investigated the real-world performance of vertically mounted bifacial PV modules on urban rooftops. The results were compelling: bifacial modules produced 10–12% more energy compared to monofacial modules despite the limited rear-side irradiance in an urban setting. This demonstrates the promise of bifacial PV even in dense and less reflective environments, particularly when careful system design is applied.

A study that compares the performance of bifacial PV modules and traditional PV modules was carried out by Raina and Sinha (2020). The study employed a modeling and simulation

methodological approach to assess the performance of monofacial and bifacial PERC PV cells. The methodological approaches involved modeling c-Si PERC bifacial solar cells under standard test conditions in different albedos using Sun Solve Software. The study compared the performance of bifacial cells to monofacial cells under these same conditions. The simulation majored in assessing the capability of c-Si PERC bifacial cells to deliver power compared to monofacial cells. This methodological approach included modeling the structure of bifacial cells by considering factors such as the anti-reflective coating (ARC) layer, front contacts, P-N junction, REA AI grid, and aluminium back surface. Additionally, the study quantified parasitic absorption losses and assessed the impact of albedo on bifacial cell output. These results were evaluated to establish the advantages of bifacial PV technologies regarding power generation and efficiency. The findings and conclusions drawn from the study are that bifacial solar cells produce more current and power compared to conventional cells, with reduced parasitic absorption losses and higher power output but at higher albedo conditions. The notable strength of this study is that it employs a simulation to assess the performance and clear presentation of the results. However, the gaps and limitations presented included the reliance on simulation data instead of experiment data and the need for further studies to validate the findings in real-world scenarios.

2.3.2 Strategies for Optimizing Bifacial Modules

Several studies have focused on strategies to optimize the performance of bifacial photovoltaic (PV) modules using a range of methodological approaches. These investigations offer insights into how bifacial gains can be maximized under varying albedo conditions, how optimization techniques can be tailored to specific site characteristics, and how to identify limitations inherent in bifacial systems.

One such study is by Marion (2021), who employed a measurement and testing approach to evaluate the reliability of satellite-derived albedo datasets in estimating bifacial PV performance. Marion compared ground-based albedo measurements from various networks and agencies with satellite-derived values. The results indicated notable discrepancies between the two data sources, raising concerns about the reliability of satellite-derived albedo when estimating energy output for bifacial systems. The study concluded that reliance on satellite-derived albedo values must be approached with caution, particularly in site-specific system design. These findings are critical as

they underscore the importance of accurate albedo measurement for precise energy yield estimation in bifacial PV systems.

A related study by Riedel-Lyngskær et al. (2022) utilized field measurements and data analysis to examine how variations in spectral albedo influence the performance of bifacial PV modules. The researchers conducted spectral irradiance measurements within the 300–1100 nm range at five-minute intervals over a 15-month period using three high-resolution EKO MS-711 spectroradiometers. Two spectroradiometers, each with a 180° field-of-view, were mounted horizontally at a height of 1.5 meters above ground level to capture comprehensive spectral data. The study found that temporal variations in spectral albedo significantly affect the energy output of bifacial systems. It highlighted that optimizing albedo characteristics could lead to improved system performance. However, the authors acknowledged that the results are highly site-specific and may not be easily generalizable to other geographic regions or environmental conditions.

Yusufoglu et al. (2015) explored the annual performance of bifacial PV modules through modeling and simulation. The study aimed to identify key optimization variables, including module tilt angle, elevation, and site-specific irradiance and albedo. Time-step simulations were used to estimate irradiance on both the front and rear sides of the modules, employing the Perez model for diffuse irradiance and Ineichen's methodology for calculating albedo. The findings revealed that energy yield increases linearly with albedo, and an optimized tilt angle could result in up to a 25% gain in energy yield. Additionally, module elevation from the ground surface significantly improved performance. The study concluded that optimization factors such as module height, albedo, and reflective surface area play critical roles in maximizing bifacial energy yield. Nonetheless, the reliance on simulation data presents a limitation, as the results may not fully reflect real-world system behaviors.

Further empirical support is provided by Saw et al. (2017), who conducted laboratory-based measurement and testing to evaluate ways to reduce bifacial cell transmittance loss. The researchers utilized glass/glass bifacial mini-modules treated with various rear-surface coatings, including infrared reflective, textured, and white reflective coatings. Sandpaper texturing was used to simulate transmittance reduction, while external quantum efficiency (EQE) measurements were taken to assess current gain. The study reported current gains of 1%, 0.3%, and 3% for infrared

reflective, textured, and white coatings, respectively. A combination of infrared and white coatings yielded a cumulative current gain of approximately 4%. These results demonstrate the potential of optical strategies to enhance bifacial performance. However, the study was conducted under standard test conditions, limiting its applicability to real-world scenarios.

Lastly, Sun et al. (2018) employed a comprehensive modeling and simulation approach to evaluate bifacial optimization strategies across different global locations with varying solar irradiance, environmental factors, and albedo levels. The study assessed multiple module configurations, including south-north, east-west vertical, and optimally tilted setups. It utilized a three-part simulation framework: a geographical-temporal irradiance model, a geometrical light-collection model, and an electro-thermal coupled model. Optimization parameters such as tilt angle, azimuth, and elevation were examined. The results indicated that raising module elevation to 1 meter and increasing albedo to 0.5 could enhance bifacial gain by up to 30%. The study also found strong agreement—within 6.4%—between simulation results and published empirical data, reinforcing the validity of the model. While the study provides useful optimization guidelines and a global perspective, it assumes idealized environmental conditions, which may limit its real-world applicability.

2.3.3 Albedo and Bifacial Performance

The influence of albedo—particularly spectral albedo—on the performance of bifacial photovoltaic (PV) modules has been a focal point of recent research. Spectral albedo refers to the wavelength-dependent reflectivity of surfaces, which affects the light available to the rear side of bifacial modules.

One significant study in this domain was conducted by Riedel-Lyngskær et al. (2022), who investigated how spectral albedo variations affect the thermodynamic efficiency limits and energy output of bifacial solar cells. The study combined theoretical modeling with high-resolution experimental data collected over a 15-month period using spectral radiometers. The findings demonstrated that spectral albedo has a marked effect on power output and should be a key consideration in solar cell design and optimization. The main strength of Riedel-Lyngskær et al.'s study lies in its methodological rigor, combining theoretical models with empirical measurements. This approach not only validated the theoretical predictions but also provided nuanced insights

into how varying spectral properties of ground surfaces can enhance or diminish the performance of bifacial modules. However, the study's limitation is its narrow scope, as the experimental setup covered only a limited range of surfaces and environmental conditions. As such, while the findings are insightful, they may not fully capture the diversity of real-world deployment scenarios.

Complementing this research, Marion et al. (2017) conducted an extensive analysis to quantify the impact of ground albedo on bifacial PV system performance using measurement-based data. The study compared satellite-derived albedo values with on-site measurements and found significant discrepancies, particularly in areas with seasonal surface changes (e.g., snow, vegetation cycles). The authors highlighted that satellite data often overestimates or underestimates real albedo conditions, thus impacting energy yield predictions. The conclusion was that accurate, ground-based albedo measurement is crucial for reliable performance modeling of bifacial PV systems.

Thus, these studies reinforce that albedo—particularly spectral and seasonal variability—is a critical variable in determining the real-world performance of bifacial PV modules. While spectral albedo directly influences thermodynamic limits and rear-side irradiation, seasonal and site-specific variability can dramatically impact long-term yield predictions. Therefore, the incorporation of accurate, site-specific, and time-resolved albedo data is essential for maximizing the performance of bifacial solar technologies, especially in diverse and dynamic environments such as those found in tropical regions.

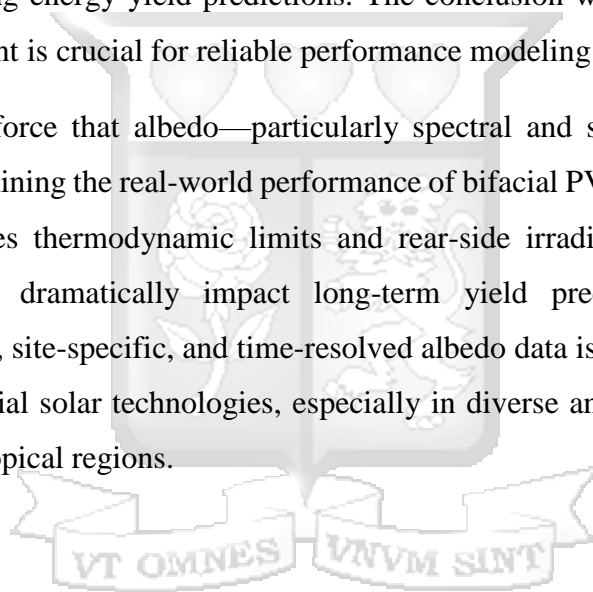
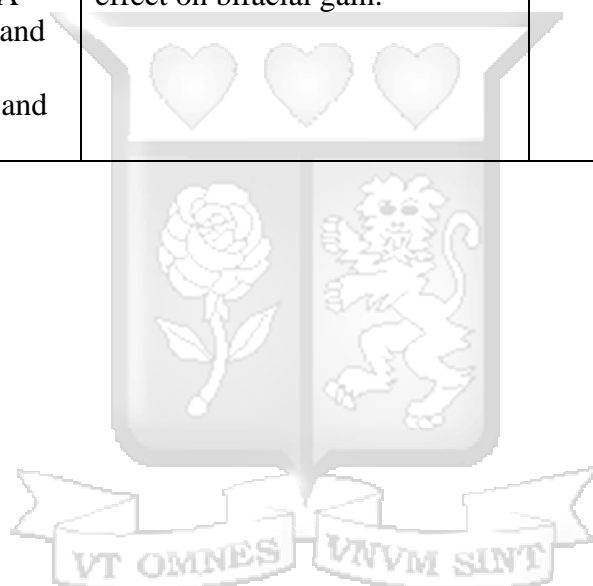


Table 2.2: Summary of Literature Review

Authors (year)	Study focus	Key findings	Gaps/limitations
Marion (2021)	Measured and Satellite-Derived Albedo Data for Estimating Photovoltaic System Performance	There is a need to validate satellite data with ground-based data to ensure accurate albedo inputs needed for performance models.	There is a need for local and high-resolution albedo datasets.
Riedel-Lyngskær et al. (2022)	The Effect of Spectral Albedo on Bifacial Photovoltaic Performance	Spectral albedo varies with ground surface type The tilt angle influences the view factor at the module's rear and impacts diffuse skylights' amount and spectral quality.	The model developed creates a lot of uncertainties around spectral measurements.
Saw et al. (2017)	Enhancing The Optical Performance of Bifacial PV Modules	Using reflective coatings in the module designs can help improve optical performance	Use of simulation data instead of real-life outdoor data The results are based on prototype-level optimization Assumptions of ideal conditions for experimental results
Raina and Sinha (2020)	Simulation Analysis of Bifacial and Monofacial PERC Solar Cells: Impact of Albedo on Performance	Increased albedo enhances bifacial PV performance. Bifacial cells benefit from environmental factors and need site-specific albedo considerations .	Limited environmental scope with data based in Amsterdam Have simplified modelling assumptions that miss out on real-world consideration
Sun et al. (2018)	Optimization and Performance of Bifacial Solar Modules: A Global Perspective	Increasing ground reflectivity from typical natural surfaces to highly reflective surfaces can boost bifacial gain by approximately 30% Elevating modules by about 1m reduces self-shading and improves bifacial performance. The optimal tilt angle tends to increase with latitude, aligning with the sun's declination and seasonal variations.	Idealized assumptions are that does not account for real-world conditions Limited local validation as the study is based on broad global data.

Yusufoglu et al. (2015)	Performance Optimization of Bifacial Solar PV Modules Under Varied Albedo Conditions	There is a linear increase in annual energy yield with higher albedo coefficients. The optimal module elevation of 1m in Cairo and 0.5m in Oslo maximizes energy yield, decreasing performance beyond the optimum.	The study is based in Cairo and Oslo, missing out on site-specific factors Lack of empirical validation
Janssen et al. (2015)	Performance Optimization of Bifacial PV Modules Considering Albedo Variation: A Modelling and Empirical Validation and Approach	Bifacial gain is significantly influenced by environmental factors such as albedo, location, and module orientation. Module temperature influences energy yields but has a minor effect on bifacial gain.	Limited scope with a focus on Amsterdam.



2.3.4 Gap Analysis of Empirical Literature Review on The Current Study

The empirical literature reveals that albedo significantly influences the energy yield of bifacial PV modules, with numerous studies demonstrating that higher albedo values can increase bifacial gain by up to 30% (Sun et al., 2018; Yusufoglu et al., 2015). Strategies to optimize bifacial module performance commonly involve increasing ground albedo through reflective surfaces and elevating modules to capture more rear-side irradiance (Riedel-Lyngskær et al., 2022; Marion, 2021). Despite these advances, several limitations and weaknesses in the existing literature highlight critical gaps that the current study seeks to address.

A consistent weakness across many studies is the heavy reliance on simulation and modeling approaches, which may not fully capture real-world variability and environmental complexities. For instance, Yusufoglu et al. (2015) based their findings predominantly on simulations, limiting the direct applicability of results to field conditions. Similarly, Sun et al. (2018) assumed idealized environmental conditions, which may not reflect actual operating environments, thus constraining the generalizability of their conclusions.

Moreover, several studies stress the necessity for extensive field measurements and empirical validation of simulation models. Marion (2021) pointed out discrepancies between satellite-derived and ground-measured albedo values, highlighting the uncertainty in performance estimations when relying solely on remote sensing data. This underlines the need for localized, ground-truth albedo data to improve bifacial PV system modeling accuracy.

Another critical gap lies in the limited exploration of temperature effects on bifacial module performance. While Janssen et al. (2015) noted temperature-related efficiency variations in bifacial modules, few studies have systematically quantified or modeled this factor, leaving a significant aspect of real-world performance unexplored.

Furthermore, the impact of spectral albedo variations has been identified as influential on bifacial PV efficiency (Riedel-Lyngskær et al., 2022), but the scope of these investigations remains narrow, often limited to specific surfaces or conditions, which restricts understanding of spectral effects across diverse environments.

In summary, although albedo and its optimization have been well-studied, key gaps persist due to the predominant use of simulations without adequate empirical validation, insufficient attention to temperature influences, and limited research into spectral albedo variations. Addressing these gaps through comprehensive field data collection and expanded parameter investigations is essential for advancing bifacial PV module performance in diverse contexts such as the tropical regions of Kenya.

2.4 Conceptual Framework

The conceptual framework of this study illustrates the relationship between key factors influencing the performance of bifacial photovoltaic (PV) modules. Figure 2.9 summarizes the relationship between the independent variables and the dependent variables. The independent variable for this study is the ground albedo (α), tilt angle (θ) and the mounting height (h). These variables are the key focus of the study as they are presumed to influence the solar PV output (the independent variable). The ground albedo was assessed using two different surfaces: the concrete surface with an albedo coefficient of 0.25-0.35 and the grass surface with an albedo coefficient of 0.15-0.25. The installation height varied from 0m, 0.5m, 1m, 1.5m, and 2m. These heights were used for each of the different surfaces. Lastly, the tilt angle was set to 15° for the experiment.

The dependent variables include the performance metrics consisting of the maximum power output (P_{max}) measured in watts, the open circuit voltage (V_{oc}) measured in voltages and the short circuit current (I_{sc}) measured in amperes. There is the fill factor (FF) measured as the ratio of maximum power output (P_{max}) to the product of the open circuit voltage (V_{oc}) and the short circuit current (I_s)

However, while the study focuses on the independent variable and its influence on the dependent variable, their effects are influenced by operational parameters and PV module characteristics. These control variables are treated as constant in assessing the influence of independent variables on the dependent variable. These variables include the parameters set by the PV module characteristics like bifaciality (δ) measured as percentage, the module area (A) measured in m^2 , and the module power temperature coefficient measured in $^{\circ}C$. The other control variable includes the environmental factors specific to the experiment site. These include the front side irradiance (G_{front}) measured in W/m^2 ambient temperature which directly affects the cell operating temperature measured in $^{\circ}C$ and standard test conditions temperature (STC) measured in $^{\circ}C$.

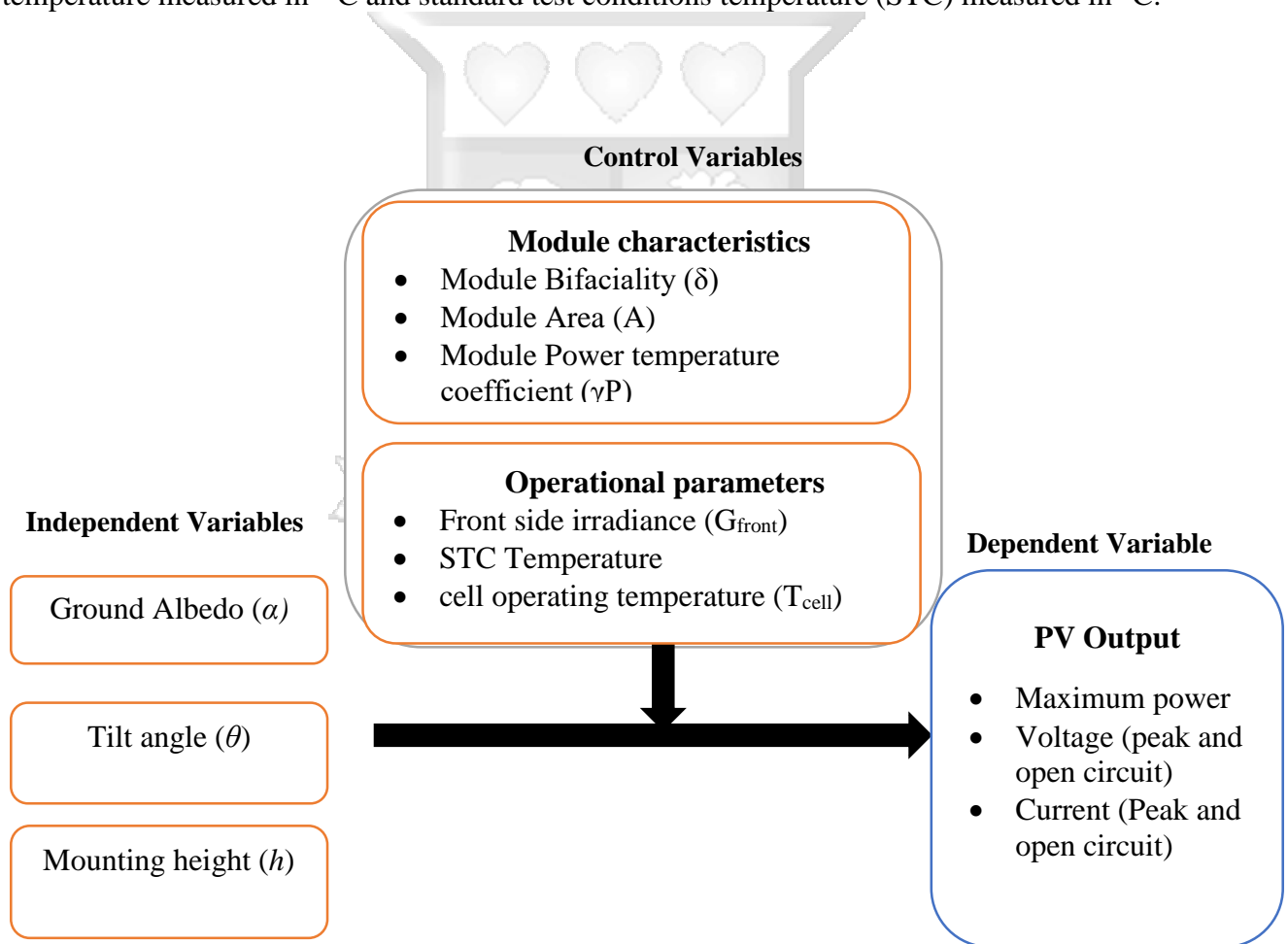


Figure 2.8: Conceptual Framework

Chapter 3: Methodology

3.1 Introduction

This chapter highlights how the study was operationalized to answer the research objectives. According to Kothari (2004), research methodology is the systematic process in which research puts into practicality the research framework developed to answer the research questions. The same ideology is supported by Asenahabi (2019), who refers to research methodology as the process through which the researcher addresses the identified research objectives. The modelling governing equations, data collection technique, data analysis process, and data collection tools are discussed.

3.2 Research Method

The research method that was adopted in this study employed empirical research. The experimental study collected data on two ground surfaces while varying the module installation height from 0m to 2m. The data was recorded to develop a predictive model that considers all the perimeters that can be used to optimize the performance of bifacial PV modules.

3.3 Experimental Setup

The experimental plan of this study was conducted in ten setups. These setups were mounted at Langata, Nairobi County, $1^{\circ}19'31''\text{S } 36^{\circ}47'22''\text{E}$. All ten setups were experimental and performed in the exact location. The ten setups involved mounting a bifacial PV module at different heights of 0m (ground level), 0.5m, 1m, 1.5m, and 2m each on concrete and grass surfaces while measuring the PV module output parameters as well as the environmental conditions affecting the performance of bifacial PV modules, which include the albedo, irradiance, and cell temperature. Table 3.1 summarizes the recorded performance outputs.

Table 3.1: Data Sheet Recorded

Data to be collected	Units
Voltage - Open-circuit voltage (V_{oc}) & Operating voltage	Volts (V)
Current - Short-circuit current (I_{sc}) & Operating current	Amperes (A)
Power - Maximum power point (P_{max}) & Instantaneous power output	Watts (W)
Irradiance	Watts per square meter (W/m^2)
Temperature – Cell	Degrees Celsius ($^{\circ}C$)
Albedo	Type of surface

3.3.1 Material and Equipment for Data Collection

The study utilized a 440W bifacial PV module and a PVA-1500 series PV analyzer to collect performance and environmental data under varying installation conditions. The following subsections provide details on the materials used.

3.3.1.1 Bifacial PV Module

A JA Solar – JAM54D41-440/LB bifacial PV module was selected for this study based on its availability and widespread use, both globally and locally in Kenya. Manufactured by JA Solar International Limited, the module features N-type bifacial cell technology, which is industry-standard, ensuring that the study's results are broadly generalizable across other bifacial PV systems.

Table 3.2 summarizes the key electrical and physical characteristics of the PV module used, including power rating, voltage, current, temperature coefficients, and bifaciality.

Table 3.2: PV Module Details

Parameter	Value	Unit
Model	JA Solar – JAM54D41-440/LB	-
P_{max}	440	W
Open Circuit Voltage (VOC)	38.90	V
Maximum Power Voltage (Vmp)	32.47	V
Short Circuit Current (Isc)	14.31	A
Maximum Power Current (Imp)	13.55	A
Module Efficiency (η)	22	%
Temperature coefficient of Isc	+0.046	%/°C
Temperature coefficient of Voc	-0.026	%/°C
Temperature coefficient of P_{max}	-0.300	%/°C
Bifaciality (δ)	80 ±10	%
Dimensions	1762±2*113±2*30±2	mm
Rated max power with 10% solar irradiation	470	W

3.3.1.2 PVA-1500 Series PV Analyser

The PVA-1500 is a specialized photovoltaic analyzer designed for field testing of PV modules. It measures I-V characteristics, irradiance, temperature, and tilt angle. Integrated software tools, including a Microsoft Excel-based Data Analysis Tool, streamline the analysis and validation of collected measurements. Table 3.3 outlines the performance specifications and technical capabilities of the PVA-1500 PV analyzer.

The PVA-1500 analyzer calibration certificate shown confirms that the equipment was calibrated on August 21, 2024 and is valid until August 21, 2026. The calibration followed procedure FPDC504.0004, in compliance with ISO 9001 and traceable to international metrology standards. Verification results show that the instrument's measurements for tilt, temperature (T1 and T2), and irradiance with AOI were all within the acceptable tolerance limits. For instance, the irradiance measurement at a nominal value of 700 W/m² yielded 666.91 W/m², well within the ±2% and ±1.5% permissible errors. All tested parameters passed, confirming the equipment's accuracy and reliability for field data collection.

Table 3.3: PVA-1500 PV Analyzer Model Characteristics

Voltage Range (voc)	20-1500V DC
Maximum current range (Isc)	0-30A DC (module efficiency <19%) 0-10DC (module efficiency ≥19%)
Voltage Accuracy (0 °C- 45 °C)	± (0.5% ±0.25V)
Current Accuracy (0 °C to 45 °C)	± (0.5% ±0.04A)
Power Accuracy (0 °C to 45 °C)	± (1.7 % + 1.0 W) (current ≥3 A, module efficiency <19 %)
Irradiance measurement range	100 W/m ² to 1500 W/m ²
Irradiance accuracy	±2 % when used to predict the performance of well-characterized poly- and monocrystalline PV modules with direct irradiance >600W/m ²
Irradiance sensor type	Silicon photodiode with corrections for temperature, spectral, and angular effects
Temperature measurement range	0 °C to 100 °C, 32 °F to 212 °F
Temperature sensor type	Type K thermocouple, two inputs
Temperature accuracy	±2 °C, 35.6 °F (not including limits of error of thermocouple)
Temperature measurement interval	Typically, 3.5 s
Tilt sensor type	Electronic
Tilt measurement range	0 to 90° from horizontal
Tilt measurement accuracy	±2° typical (0 to 45°)

Source: Fluke (2023)

3.3.2 Testing Procedure

The primary objective of the testing procedure was to evaluate the impact of module height, surface albedo, and tilt angle on the output performance of bifacial PV modules. The procedure was implemented consistently across all ten setups to ensure comparability and accuracy of results.

3.3.2.1 Module Height

Module height was the primary independent variable in the study. PV modules were mounted at five discrete height levels: 0 m, 0.5 m, 1 m, 1.5 m, and 2 m using an adjustable racking system that allowed for uniform testing. Each height configuration was tested independently on both concrete

and grass surfaces, with data collected from 11:00 AM to 1:00 PM, a period selected for high solar irradiance consistency.

3.3.2.2 Tilt Angle

All PV modules were fixed at a 15° tilt angle, which is optimal for the geographical location of Nairobi. The tilt was measured and confirmed using the tilt sensor of the PVA-1500 analyzer, this ensured precision across all configurations.

3.3.2.3 Fill Factor

The fill factor (FF) is a measure of the PV module's electrical quality and is used to assess the "squareness" of its I–V curve. According to Nelson (2003), FF is mathematically defined as:

$$FF = \frac{I_{mp} \times V_{mp}}{I_{sc} \times V_{oc}}$$

3.1:

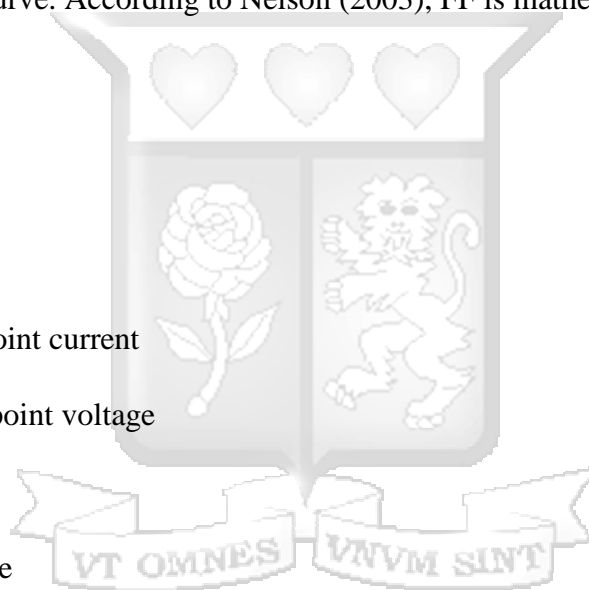
Where;

I_{mp} = Maximum power point current

V_{mp} = Maximum power point voltage

I_{sc} = Short circuit current

V_{oc} = Open-circuit voltage



This metric provided insight into the internal resistive losses and overall efficiency of the PV module under various installation conditions.

3.3.2.4 Data Collection

Primary data was recorded using the PVA-1500 analyzer. The tool automatically captured irradiance, module temperature, current, voltage, and real-time power output. Data was validated using the associated analysis software, and recordings were taken at regular intervals throughout each testing session.

3.4 Inclusion/Exclusion Criteria

This research adopted a purposive sampling strategy. This sampling approach uses the study population based on their availability and convenience to the research objective. Precycle in the context of this research, purpose sampling was deemed the most appropriate approach as the study is specific to the performance of bifacial PV modules in Kenya. This ensured the manipulation of various albedo conditions and setting up the bifacial solar PV modules at varying heights of 0m to 2m, typical of installations in Kenya. Additionally, the PV module's selected size is based on availability and is the most widely used in Kenya for residential and commercial applications. The performance of the PV module and the factors affecting its performance were recorded instantaneously at every setup.

3.5 Reliability and Validity of Research Instruments

3.5.1 Data Analysis

This study sought to formulate a performance optimization model for bifacial solar PV modules under varied albedo conditions. Excel Solver was used for the modelling to get the best setup parameters to increase energy yield for bifacial PV modules in different albedo conditions and varied installation heights. First, the experimental test results were used to evaluate the optimal values and conditions for the different parameters. This study used the frameworks Yusufoglu et al. (2015) developed to model irradiance reaching the rear surface and the Perez model for estimating solar irradiance on a tilted surface.

3.5.2 Modeling for Irradiance Reaching the Rear Surface

Like the irradiance parameter, module installation factors such as height and orientation were recorded. Environmental factors such as albedo, solar Irradiance, and cell temperatures are more critical. With these parameters in hand, the model formulated by Yusufoglu et al. (2015) as a framework for irradiance reaching the rear surface was used as a foundation framework to inform the model arrived at in this study. According to the model created by Yusufoglu et al. (2015), the essential factors to consider are the nature of sources of light (direct sunlight, diffuse sunlight, and ground-reflected sunlight). The model also includes the calculation of direct and diffuse irradiance and the determination of the view factor.

3.5.3 Data Preparation and Exploratory Data Analysis

Data consistency and reliability were ascertained using the PVA-1500 Data analysis tool, which automatically and consistently recorded the variable data. The inbuilt data analysis tool ensured no mishaps were associated with manual recording and analysis. The raw data were exported into an Excel file for further processing and analysis.

3.5.4 Model Development

The results obtained from the data analysis tool and the exploratory results employed a nonlinear regression optimization approach. This optimization sought to maximize energy yield by balancing mounting height against thermal and other installation criteria. Elevating modules increases rear-side irradiance by improving the view factor using the equation. Equation 3.1 illustrates how to determine the view factor

$$F_{g(h,\theta)} = F_{max} \cdot \left(1 - e^{-\frac{h \cdot \cos\theta}{H_0}} \right)$$

3.2

Where:

$F_{g(h, \theta)}$: View factor from the rear side of the PV module to the ground

F_{max} : Represents the maximum theoretical rear-side exposure to ground-reflected irradiance for a flat, tilted surface (typically 0.5)

h : Module height above ground (m)

θ : Tilt angle of the module (degrees or radians)

H_0 : Characteristic height where 63% of F_{max} is reached (m)

This formula is adapted from simplified radiative view factor principles described in Marion et al. (2017) and Deline et al. (2012) and mirrors the exponential height saturation behaviour observed in empirical models like those proposed by Castillo-Aguilella & Hauser (2016) and PVsyst's bifacial irradiance modelling framework. The maximum view factor $F_{max}=0.5$ arises from

classical radiative geometry, where a flat surface facing a semi-infinite ground plane "sees" half the hemispherical field of view, as discussed in Incropera et al. (2007) and Modest (2013). The parameter H_0 represents the characteristic height at which bifacial rear irradiance substantially saturates, and it is used in empirical and semi-analytical models derived from view factor theory by (Deline et al., 2012) and Castillo-Aguilella & Hauser (2016).

The view factor formula helps quantify ground-reflected light captured by the rear surface (Deline et al., 2018). Notably, heightening modules introduces diminishing effects in $F_g(h, \theta)$, temperature-related power losses due to higher cell temperatures (T_{cell}), reduced efficiency via voltage drops, and net power degradation (King et al., 2004; Mikofski et al., 2020). Thus, the optimization model integrates these competing effects to identify the height (h) that maximizes power output.

The combined equation for optimization is given below:

$$P = \left(\eta \cdot A \cdot \left[G_{front} + \delta \left(G_{front} \cdot \alpha \cdot F_{max} \cdot \left(1 - e^{-\frac{h \cdot \cos \theta}{H_0}} \right) \right) \right] \right) \cdot \left[\frac{100 + (\gamma P \cdot \Delta T)}{100} \right]$$

Equation 3.3: Performance Output Predictive Model

Where:

P is the maximum power output of the module

H is the module efficiency

A is the module area

G_{front} is the irradiance on the front side (assumed constant for fixed tilt/orientation)

δ is the bifaciality factor

α is the Ground albedo reflectance

F_{max} is the maximum theoretical rear-side exposure to ground-reflected irradiance for a flat, tilted surface (typically 0.5)

h is the mounting height

θ is the tilt angle of the module (degrees)

H_0 is the characteristic height where 63% of F_{\max} is reached (m)

γP is the Power temperature coefficient (%/°C)

ΔT is the difference between cell operating temperature (T_{cell}) and STC temperature ($T_{\text{STC}}=25^\circ\text{C}$).

This equation was used to check out the experiment's performance parameters. If all the parameters were factored in and the formula was worked out, would the power output be close to the one established in the experiment. This function was then converted to a maximization problem with mounting height and albedo values as decision variables, while other variables were fed in as constants.

3.6 Ethics in Research

This study was firmly committed to upholding the highest ethical standards outlined by the Strathmore University research guidelines. To ensure ethical conduct, all necessary documentation was submitted to the Strathmore University Institutional Scientific and Ethics Review Committee (SU-IERC) for comprehensive review. This work was conducted following the university's ethical research provisions. Full disclosure of the data's uses helped enhance the process's ethicality. The research aims to contribute to a robust and responsible knowledge base within the field by adhering to these established ethical frameworks.

3.7 Dissemination of Results

The study findings will be disseminated through various platforms to make them accessible to the public. The first presentation will be during the Strathmore University research defence session. The session will have the University's academic expert panel evaluate the study and its relevance. After that, the final report will be published in the university's repository and accessible to the academic fraternity.

3.8 Utilization of Research

The study's findings will create insights into optimizing installations for optimal performance for solar systems using bifacial modules. The evaluated factors and model developed will help engineers and designers create more efficient solar installations that maximize energy production under varying albedo conditions. The information will be crucial to investors, project developers, and policymakers in making informed decisions on the financial viability of bifacial solar projects. Regulatory bodies such as the Energy and Petroleum Regulatory Authority (EPRA) will use the outcomes to improve the inspection and certification processes, ensuring that solar installers and contractors adopt optimal standards.



Chapter 4: Results And Discussion

4.1 Introduction

This chapter presents performance results for bifacial PV modules tested under different conditions. The chapter is divided into three sections. The first section presents the performance results of the bifacial PV module when tested under different albedo conditions and varying installation heights. The second section presents the model development and the optimization function as well as testing, and the final section covers the discussion as relevant to the research objectives.

4.2 Experimental setup

The experiment was conducted at Langata, whose coordinates are $1^{\circ}18'37.44''\text{S}$, $36^{\circ}48'51.84''\text{E}$. Figures 4.1,4.2,4.3 and 4.5 illustrate the mounting stand design used for all the experiments. All measurements are given in millimetres. The tilt angle was set at 15° for all the experiments. The decision to work with a 15° tilt angle comes from the rule of the thumbs, as discussed by Abdeen et al. (2017), elaborates that the optimal tilt angle is based on the site's latitude added or subtracted to 15° depending on the seasonal variations of the sun's location. Because the site of this study is just above the equator line, the study found 15° to achieve the balance between self-cleaning capabilities and maximum irradiance. Mousazadeh et al. (2009), Found that dust losses increase significantly when tilt drops below 15° .

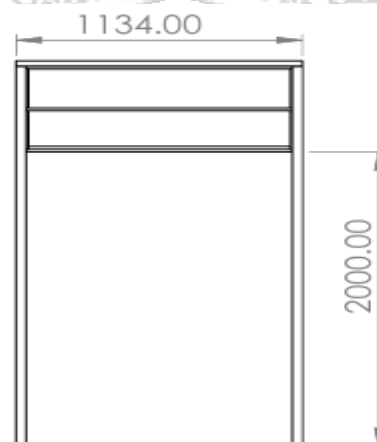


Figure 4.1: Mounting Stand Side view dimensions

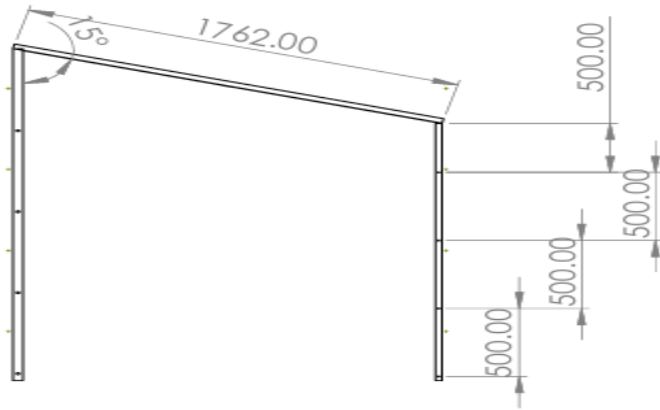


Figure 4.2: Mounting stand adjustable Levels

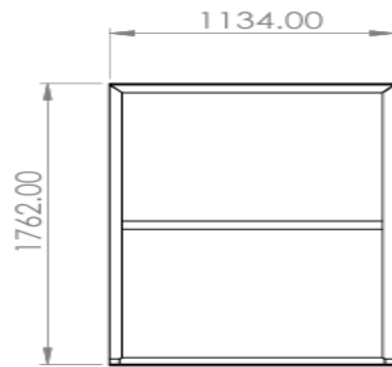


Figure 4.3: Top view dimensions



Figure 4.4: 3D Illustration

4.2.1 Bifacial Solar PV Module Setup on Concrete Surface

The experiment was conducted on 21st January. The measurements were taken and recorded in real time between 11.18 AM and 12.23 PM. The general weather condition at the time of the experiment was cloudy with a temperature of 27°C, humidity of 27% and 13.7km/h Northeasterly winds. Table 4.1 summarizes the timeline for the experiment through the different mounting levels.

Table 4.1: Experiment Timelines for Concrete Surface Setup

Height Level (m)	Date	Time (GMT+3)	Albedo factor value (concrete)
0	1/21/2025	11:18:08 AM	0.25-0.35
0.5	1/21/2025	11:33:35 AM)	0.25-0.35
1	1/21/2025	11:52:40 AM	0.25-0.35
1.5	1/21/2025	12:07:20 PM	0.25-0.35
2	1/21/2025	12:23:49 PM	0.25-0.35

The concrete used was a partially smooth slab with a shiny surface and grey in colour, as shown in Figure 4.5. For each mounting level, 500 readings were made and recorded. Two thousand five hundred measurements were taken for the solar system on the concrete surface setup.



Figure 4.5: Bifacial PV Module Mounted on a Concrete Surface

4.2.2 Solar System on Grass Surface

The experiment was conducted on 3rd March 2025. The measurements were taken between 12.09 PM and 1.17 PM. The general weather conditions during the experiment were a cloudy day, a

temperature of 28°C, 29% humidity, and 23km/hr easterly winds. The timing of the readings and measurements are summarized in Table 4.2

Table 4.2: Experiment Timelines for Grass Surface Setup

Height level (m)	Date	Time (GMT+3)	Albedo factor value (concrete)
0	3/3/2025	12:09:37 PM	0.14-0.25
0.5	3/3/2025	12:25:55 PM	0.14-0.25
1	3/3/2025	12:41:02 PM	0.14-0.25
1.5	3/3/2025	1:01:57 PM	0.14-0.25
2	3/3/2025	1:17:08 PM	0.14-0.25

The type of grass surface used is early sprouting; 500 readings were made and recorded for each mounting height level. Figure 4.6 illustrates the setup.



Figure 4.6: Bifacial PV Module Mounted on a Grass Surface

4.3 Data Presentation

Section 4.3 presents the actual performance measurements recorded from the bifacial PV module under the varying setups as discussed in chapter 3.

4.3.1 Performance Output on Concrete Surface Setup

The module's height above ground was varied at five levels (0m, 0.5m, 1.0m, 1.5m, and 2.0m), reflecting common installation practices in Kenya, where heights beyond 2.0m are limited by structural and economic constraints. Measurements were recorded using a PVA-1500 PV analyzer at 1.5-second intervals, capturing 2,500 total data points—500 per height level. Assumptions included constant front-side irradiance for the short duration of data collection, uniform surface albedo, negligible wind effects due to calm conditions, and that a single-panel setup was adequate for analyzing relative performance trends

Table 4.3: PV Module Performance Results by Height Level on Concrete Surface

Height level (m)	Irr (W/m ²)	I _{sc} (Amps)	Temp (°C)	Voc (volts)	I _{mp} (Amps)	V _{mp} (volts)	P _{max} (watts)	FF
0	865	12.92	63.3	36	11.67	28	325	0.69
0.5	891	14.3	53	37	13.41	28	373	0.71
1	890	14.69	64.8	37	13.79	29	397	0.73
1.5	847	15.51	60.8	37	14.79	29	428	0.74
2	932	15.28	58.4	37	14.98	29	432	0.76

Table 4.3 presents the performance metrics of the solar system installed at varying heights above a concrete surface. The irradiance (Irr) values across all five height levels are relatively consistent, ranging from 847 W/m² to 932 W/m², with the highest irradiance recorded at 2 meters. This slight variability is attributed to natural fluctuations in sunlight during the one-hour measurement window. A clear trend is observed in the short circuit current (I_{sc}), which generally increases with mounting height—from 12.92 A at 0 m to a peak of 15.51 A at 1.5 m—before a slight decrease to 15.28 A at 2 m. This trend suggests enhanced backside irradiance capture due to increased ground clearance and reflective contribution from the concrete surface. The dip at 2 m may be due to momentary atmospheric changes or partial shading during that interval. Temperature readings remained relatively stable across all height levels, averaging between 53°C and 64.8°C, indicating that elevation had minimal influence on thermal behavior during the short measurement period.

Similarly, the open circuit voltage (Voc) values remained stable across all height levels, ranging from 36 V to 37 V, showing that module elevation had negligible impact on voltage output. The maximum power current (I_{mp}) increased consistently with height, from 11.67 A at 0 m to 14.98 A at 2 m, correlating strongly with observed gains in power output (P_{max}), which rose from 325 W at 0 m to 432 W at 2 m. This trend implies improved energy harvesting efficiency with increasing elevation. Furthermore, the fill factor (FF) also improved with height, increasing from 0.69 at ground level to 0.76 at 2 m. This suggests better module performance and internal efficiency as height increases.

4.3.2 Performance Output on Grass Surface Setup

Similar to the case of concrete surface, a total of 500 instances of recording was done and table 4.6 summarizes the recordings.

Table 4.4: : PV Module Performance Results by Height Level on Grass Surface

Height level (m)	Irr (W/m²)	I_{sc} (Amps)	Temp (0C)	Voc (volts)	Imp (Amps)	Vmp (volts)	P_{max} (watts)	FF
0	938	13.92	77.2	35	12.55	26	332	0.68
0.5	948	14.88	70	36	13.72	26	363	0.68
1	947	14.91	71.4	36	13.71	26	363	0.68
1.5	942	15.36	72.3	36	14.64	26	382	0.70
2	949	15.59	70.9	36	14.02	28	389	0.69

According to Table 4.4, the irradiance values across the different height levels are also fairly consistent, with the highest value registered at 2m. Natural fluctuations in sunlight could also explain the slight variations in irradiance level. As for the Short circuit current (I_{sc}), there is also a general trend of increasing I_{sc} with increasing height, with 13.92 registered at 0m and 15.59A at 1.5m. Therefore, there is a general implication of improving the current generation with increasing mounting height, which suggests increased backside irradiance from a wider reflective area. About the cell temperature, the results show a relatively stable temperature across the height levels with even more minor variations. This also implied that the mounting height did not cause significant temperature variations. As for the open circuit voltage, there is an even more stable measurement across the different heights.

Similarly, the maximum power current seems to increase with height, with 12.55Amps registered at 0m and 14.00Amps registered at 2m; as for the maximum power output, there is also a general trend in power increase with increasing height. Starting with 332W at 0m and 389W at 2m. The performance factor also shows an increase in the mounting height, further suggesting a general increase in power transfer efficiency with height for concrete surfaces. Lastly, the fill factor is high across all height levels, with a slight rise in mounting height, suggesting that mounting higher height influences cell efficiency improvement.

4.3.3 Solar PV module on Concrete and Grass Surfaces Power Output Comparison

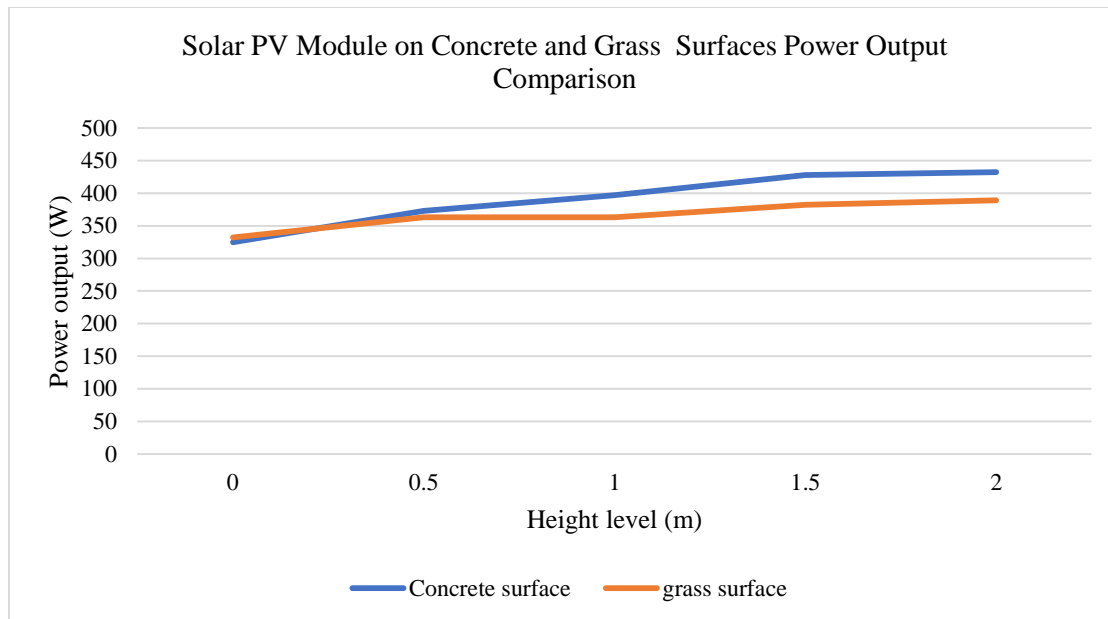


Figure 4.7: Concrete and Grass Surfaces Power Output Comparison

From Figure 4.7, it is evident that there is an upward trend in energy output as mounting height increases for both surface types. Notably, the concrete surface has a higher power output and height than the grass surface. A case in point is a minimal difference at ground-level mounting but a substantial difference at 1.5m height. These differences are attributed to higher albedo values of concrete surfaces (0.25-0.35) than grass surfaces (0.14-0.25). The implication is that increasing mounting height is more pronounced on the concrete surface, showing that albedo and mounting height influence power output. The highest output for a solar system on a concrete surface is achieved at 1.5m with 432W energy output; the highest output for a grass surface is achieved at 2m with 389W.

4.3.4 Irradiance Comparison between Solar PV modules on Concrete and Grass Surface

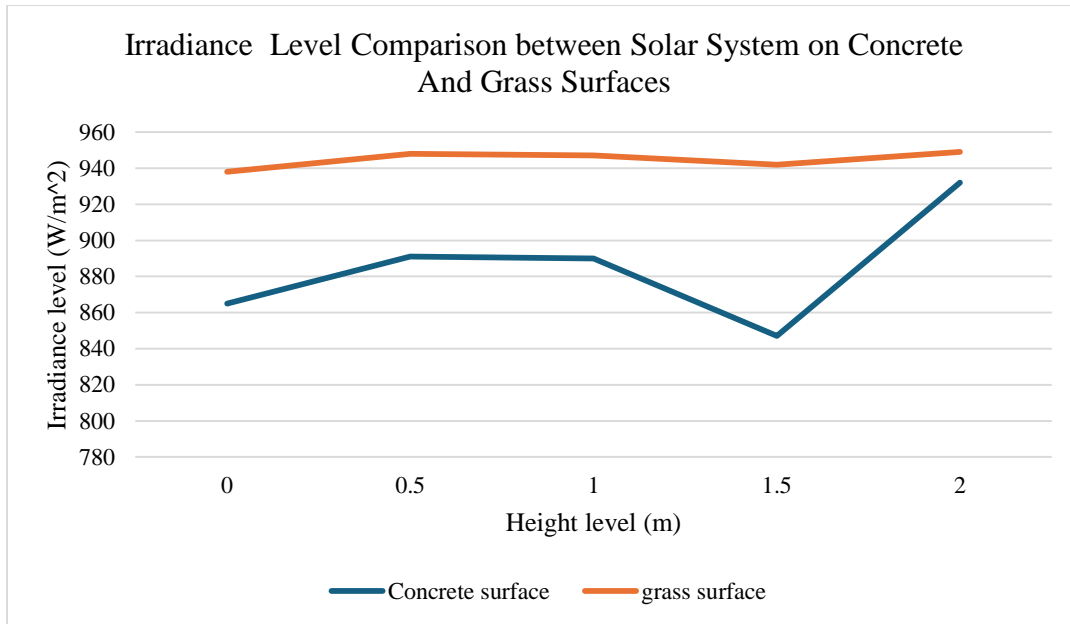


Figure 4.8: Irradiance Level Comparison Between Concrete and Grass Surface

Figure 4.8 shows that irradiance levels for grass surfaces are consistently high, with a range of 938 W/m² and 949 W/m². There is also minimal variation in irradiance level across different mounting heights. As for the concrete surface, there is notably higher variation across the experiment time with a range of 847 W/m² and 932 W/m². Notably, the irradiance values of the concrete surface are generally lower than that of the grass surface except at 2m height.

What is important to note is that there is a time difference in the time of the experiments. The concrete surface measurements were taken on January 21, 2025, between 11:18 AM and 12:23 PM. The grass surface measurements were taken on March 3, 2025, between 12:09 and 1:06 PM. The implications are that the grass surface measurements were taken closer to solar noon, which can account for consistently high irradiance values. The time differences imply that each test's solar angle changed at different rates. Besides, the concrete surface measurements were taken over a comparably wider time window, which can account for variation in irradiance. Another critical factor is that the experiment location, Nairobi, near the equator, could imply a relatively consistent solar irradiance throughout the year. Thus, the difference in dates could have contributed to a negligible impact on differences in solar irradiance.

4.3.5 Cell Temperature Comparison between PV Module on Concrete and Grass Surface

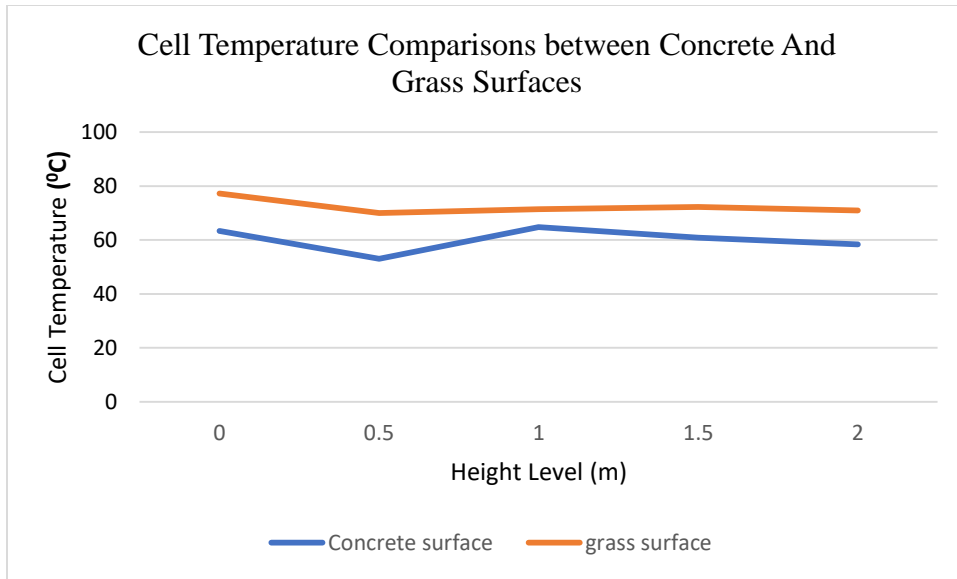


Figure 4.9: Cell Temperature Comparisons Between Concrete and Grass Surfaces

Figure 4.9 shows that the cell temperature values for grass surfaces are consistently higher than those of concrete surfaces (70°C to 77.2°C and 53°C to 64.8°C respectively). Notably, there is a slight variation in cell temperature for different mounting heights in the case of grass surfaces. In contrast, concrete surfaces show slightly more variation across the various heights. The timing of the experiment explains the higher cell temperature in the grass surface. First, it was taken in March, during which Nairobi typically experiences higher temperatures than January. Secondly, the time window of the grass surface test was done at the hotter time of the day compared to when the measurement of the concrete surface was taken (late morning hours towards noon). It is worth noting that the PV output decreases with an increase in cell temperature; the temperature coefficient is listed in Table 3.2.

4.3.6 Fill Factor Comparison between Solar PV Module on Concrete and Grass Surface

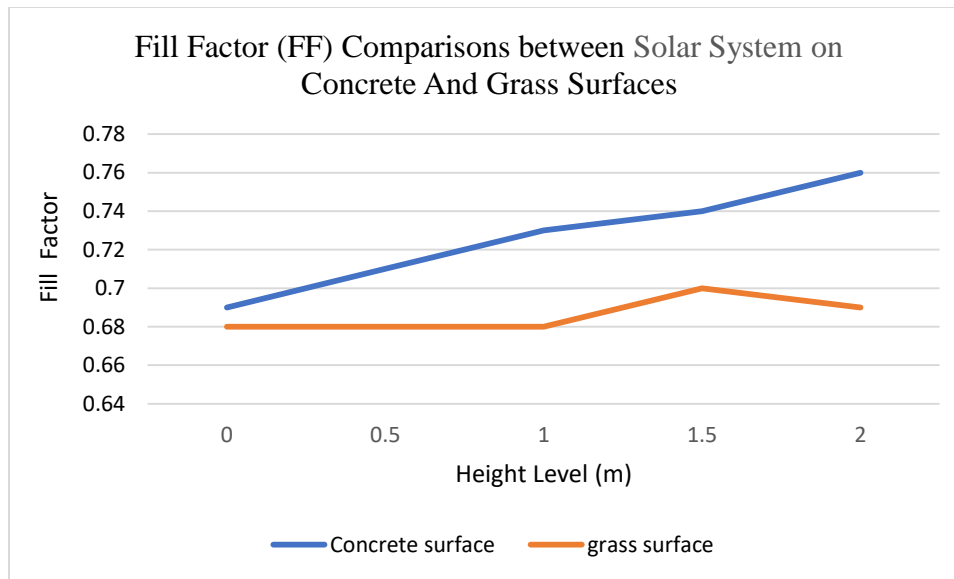


Figure 4.10: Fill Factor (FF) Comparison Between Concrete and Grass Surface

Figure 4.10 shows that the concrete surface has a consistent upward trend with an increase in mounting height between 0.69 and 0.76. whereas grass surface has relatively stable values ranging from 0.68 to 0.70, there is negligible variation between different height levels. The implication is that a higher albedo combined with height values positively influences the fill factor.

4.4 Model Development

4.4.1 Testing the Predictive Model

To test the predictive model shown in equation 3.2 to check the performance parameters, the calculations are based on figures from Table 4.3, which focus on a 2m mounting height with the solar PV module on the concrete surface.

$$\eta = 22\% \text{ (Table 3.2)}$$

$$A = 1.99801\text{m}^2 \text{ (Table 3.2)}$$

$$G_{\text{front}} = 932 \text{ W/m}^2 \text{ (Table 4.4)}$$

$$\delta = 80\% \text{ (Table 3.2)}$$

$$\alpha = \frac{0.25+35}{2} = 0.3 \text{ (Table 2.1)}$$

$$F_{max} = 0.5$$

$$h = 2\text{m (Table 4.4)}$$

$$\theta = 15^{\circ}$$

$$\gamma P = -0.300\% / ^{\circ}\text{C (derived from PV module characteristics from Table 3.2)}$$

$$\Delta T = (58.4^{\circ}\text{C} - 25^{\circ}\text{C}) = 33.4^{\circ}\text{C}$$

Thus, substituting the variables with values:

$$P = \left(0.22 \cdot 1.99801\text{m}^2 \cdot \left[932\text{Wm}^{-2} + 0.8 \left(932\text{Wm}^{-2} \cdot 0.3 \cdot 0.5 \cdot \left(1 - 2.71828183 \left(\frac{2\text{m} \cdot \cos 15^{\circ}}{0.63 \cdot 0.5\text{m}} \right) \right) \right) \right] \cdot \left[\frac{100 + (-0.3^{\circ}\text{C}^{-1} \cdot 33.4^{\circ}\text{C})}{100} \right] \right) \approx 412.50\text{W}$$

The Predicted P_{\max} of 412W is 4.51% less than the measured P_{\max} of 432W. The -4.51% deviation can be accounted for by missing out on other parameters that influence the overall output of PV modules.

Alternatively, using the values from Table 4.4 (solar PV module on a grass surface)

$$\eta = 22\% \text{ (Table 3.2)}$$

$$A = 1.99801\text{m}^2 \text{ (Table 3.2)}$$

$$G_{\text{front}} = 949 \text{ W/m}^2 \text{ (Table 4.6)}$$

$$\delta = 80\% \text{ (Table 3.2)}$$

$$\alpha = \frac{0.14+0.25}{2} = 0.195 \text{ (Table 2.1)}$$

$$F_{max} = 0.5$$

$$h = 2\text{m (Table 4.4)}$$

$$\theta = 15^{\circ}$$

$$\gamma P = -0.300\% / ^{\circ}\text{C (Table 3.2)}$$

$$\Delta T = (70.9^{\circ}\text{C} - 25^{\circ}\text{C}) = 45.9^{\circ}\text{C}$$

$$P = \left(0.22 \cdot 1.99801m^2 \cdot \left[949Wm^{-2} + 0.8 \left(949Wm^{-2} \cdot 0.3 \cdot 0.5 \cdot \left(1 - 2.71828183 \left(\frac{2m \cdot \cos 15^\circ}{0.63 \cdot 0.5m} \right) \right) \right) \right] \cdot \left[\frac{100 + (-0.3^\circ C^{-1} \cdot 45.9^\circ C)}{100} \right] \right)$$

≈387.535W

To evaluate the accuracy of the predictive model introduced in Equation 3.2, performance parameters were tested using data from Table 4.3, specifically focusing on the solar PV module mounted at a 2-meter height on a concrete surface. Substituting relevant values—including an efficiency (η) of 22%, panel area (A) of 1.99801 m², front irradiance (G_{front}) of 932 W/m², bifaciality factor (δ) of 80%, albedo (α) of 0.3, and thermal coefficient (γ_P) of -0.3%/°C—the predicted power output was calculated as approximately 412.5 W. When compared to the actual measured maximum power (P_{max}) of 432 W at the same height, this prediction deviated by -4.51%. This discrepancy may be attributed to simplified modeling assumptions, including exclusion of factors such as ambient wind cooling, panel soiling, electrical mismatch losses, and real-world variability in albedo or irradiance diffusion, which collectively impact overall module performance.

A similar analysis was conducted using values from Table 4.4, which documents performance for the same PV module mounted at 2 meters over a grass surface. In this case, the model predicted a P_{max} of 387.5 W, closely matching the measured output of 389 W with only a -0.38% deviation. The minimal discrepancy here suggests that the model performs more accurately under lower-reflectance surfaces like grass, potentially due to reduced sensitivity to reflected irradiance variations. This further confirms the model's robustness in standard conditions and highlights the value of accounting for mounting height, surface albedo, and temperature in bifacial PV performance estimation. However, future refinements could improve accuracy by incorporating more dynamic albedo models and real-time environmental feedback.

Table 4.5 further compares the predictive model's results against the measurements taken.

Table 4.5: Performance Optimization Formula Test for Different Surfaces and Mounting Height Levels

Height level (m)	Concrete surface ($\alpha = 0.3$)			Grass surface ($\alpha = 0.195$)		
	predicted P_{max} (W)	Measured P_{max} (W)	Dev.	predicted P_{max} (W)	Measured P_{max} (W)	Dev.
0	336.534	325	3.55%	347.742	332	4.74%
0.5	388.911	373	4.27%	380.146	363	4.72%
1	382.133	397	-3.74%	383.764	363	5.72%
1.5	371.131	428	-13.29%	382.282	382	0.07%
2	412.502	432	-4.51%	387.535	389	-0.38%
Average deviation			-2.75%			2.98%

The average deviation of -2.75% for the concrete surface suggests that the model generally falls slightly below the measured value. This systematic underprediction could be explained by not accounting for variables like wind speed direction, soiling and shading effects, relative humidity, and spectral irradiance distribution. The same can be said about a 2.98% deviation in the grass surface. However, the very low deviation values suggest that the model can still provide an essential basis for developing a predictive model for albedo and mounting height for maximum power output. Figures 4.11 and 4.12 further summarize this data.

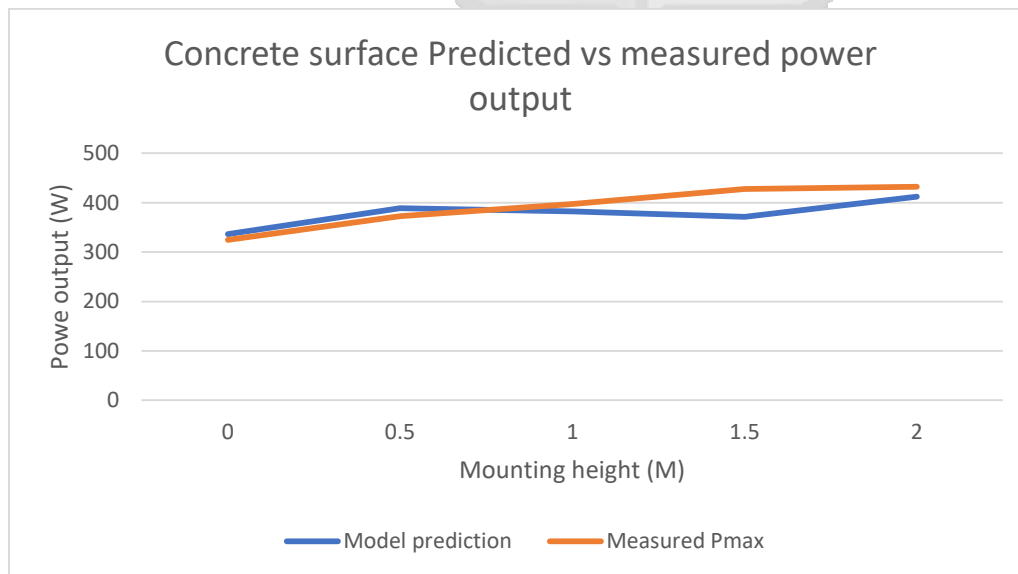


Figure 4.11: Concrete Surface Predicted Output Measured Power Output

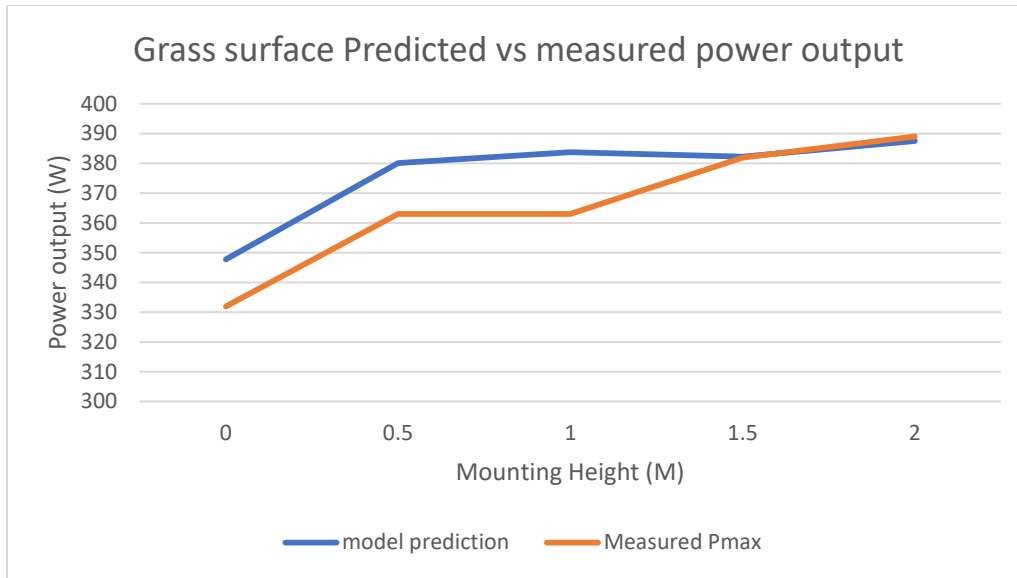


Figure 4.12: Grass Surface Predicted Output Measured Power Output

4.4.2 Developing Optimization Model

The performance optimization model generally tries to optimize the view factor. According to Yusufoglu et al. (2015), the view factor of solar module installation is primarily influenced by the mounting height and the tilt angle; the higher the view factor, the higher the performance. Therefore, this model tries to find the optimum mix of installation height and the tilt angle; this, coupled with the highest attainable surface albedo, would provide the optimum output under the provided site-specific and PV module parameters.

The performance optimization model is developed by changing the predictive model into a maximization objective function. The objective function uses the albedo coefficient, the mounting height, and the tilt angle as decision variables. Since the maximum rated power of the module used is 475W, the objective was set to maximize the value of 475.

4.4.2.1 Decision variables

4.4.2.1.1 Albedo Coefficient (α)

The albedo coefficient is a ratio between 0 and 1. Therefore, the constraints are set to at least zero but not more than 1.

4.4.2.1.2 Mounting Height (h)

The mounting height is constrained between ground level (0m) and 2 meters. The decision to have maximum mounting height at 2m balances the cost aspects of mounting structures, manual cleaning, and subjecting mounting structures to adverse weather conditions like wind. Additionally, 2m is the most common maximum mounting height.

4.4.2.1.3 Tilt Angle (θ)

The tilt angle constraints are equal to or more than 0° and equal to or less than 15° . The constraints are based on Yusufoglu et al. (2015) and Abdeen et al. (2017) recommendations on the optimum tilt angle based on the site's location and latitude.

4.4.2.2 Objective Function

Optimize P to a value of 475, which is the modules maximum output;

$$P = \left(\eta \cdot A \cdot \left[G_{front} + \delta \left(G_{front} \cdot \alpha \cdot F_{max} \cdot \left(1 - e^{-\frac{h \cdot \cos \theta}{H_0}} \right) \right) \right] \right) \cdot \left[\frac{100 + (\gamma P \cdot \Delta T)}{100} \right]$$

Subject to:

- i. $0 \leq h \leq 2$
- ii. $0 \leq \alpha \leq 1$
- iii. $0 \leq \theta \leq 15$

Microsoft Excel's Solver tool was used to work out the objective function and find the optimum solutions for the decision variables. Figure 4.13 illustrates the Solver's framework.

Parameters	Optimal values	
Module efficiency (η)	0.22	Module Specifications Data
Module Area (A)	1.998	Module Specifications Data
Front side irradiance (G_{front})	884	Measured Data
Module Bifaciality (δ)	0.80	Module Specifications Data
Surface albedo reflectance (α)	0.961	Decision Variable
Maximum theoretical rear-side exposure to ground-reflected irradiance (F_{max})	0.500	Assumed Constant
Module Mounting Height (h)	1.26	Decision Variable
Tilt angle (θ)	10.84	Decision Variable
Characteristic height where 63% of F_{max} is reached (H_0)	0.32	$= 0.63 \cdot F_{max}$
Module Power temperature coefficient (γP)	0.300	Module Specifications Data
STC temperature	25.00	Assumed
Cell operating temperature (T_{cell})	60.60	Measured
Temperature difference between cell and operating temperature (ΔT)	35.60	$= T_{cell} - STC$
view factor	0.9663	$= 1 - e^{-\frac{h \cdot \cos \theta}{H_0}}$
Power coefficient from output loss due to cell temperature	0.8932	$= \frac{100 + (\gamma P \cdot \Delta T)}{100}$
Output power (Pmax)	474.088	<p><i>objective function:</i></p> $\text{maximize } P = \left(\eta \cdot A \cdot \left[G_{front} + \delta \left(G_{front} \cdot \alpha \cdot F_{max} \cdot \left(1 - e^{-\frac{h \cdot \cos \theta}{H_0}} \right) \right) \right] \right) \cdot \left[\frac{100 + (\gamma P \cdot \Delta T)}{100} \right]$

Figure 4.13: Excel's Solver Parameters Framework

The objective function aimed to optimize the maximum power output (P) to a target value of 475 W by adjusting key decision variables—mounting height (h), surface albedo (α), and tilt angle

(θ)—within specified constraints ($0 \leq h \leq 2$ m, $0 \leq \alpha \leq 1$, $0^\circ \leq \theta \leq 15^\circ$). Using Microsoft Excel's Solver tool, the optimization process identified the optimal combination of parameters that maximize power output, as detailed in Figure 4.13. The solution yielded a module efficiency (η) of 0.22, module area (A) of 1.998 m², front irradiance (G_{front}) of 884 W/m², bifaciality factor (δ) of 0.80, and a high surface albedo reflectance (α) of 0.961. The optimum mounting height was found to be 1.26 m, with a tilt angle of 10.84°, and a characteristic height (H_0) of 0.32 m where 63% of the maximum theoretical rear irradiance ($F_{\text{max}} = 0.5$) is reached. Cell operating temperature was optimized at 60.6°C, resulting in a temperature difference (ΔT) of 35.6°C and a power temperature coefficient adjustment factor of 0.8932. The resulting view factor was 0.9663, leading to an optimized maximum power output (P_{max}) of approximately 474.1 W, closely matching the target and demonstrating the effectiveness of the Solver in balancing physical and environmental parameters to maximize module performance.

4.4.3 Testing the Optimization Model

The optimization model was tested using site measurements from the solar PV module on the concrete and grass surfaces from Table 4.3 and Table 4.4, respectively. The figures are from the mean measurements taken while experimenting with the solar module on both surfaces (the averages for all mounting levels).

4.4.3.1 Testing with Solar PV module on Concrete Surface

Other than the solar module's specification data, the data measured on-site were irradiance and cell operating temperatures. As such, assuming that the mean cell operating temperature for the site was 60.6°C and the irradiance level was 884 W/m². The optimal albedo conditions would be a surface reflectance of 0.961, a tilt angle of 10.84°, and a module mounting height of 1.26m. Assuming all other factors are constant, the optimal power output would be 474.088W. Table 4.6 summarizes the optimal parameters and output.

Table 4.6: Optimum Albedo, Mounting Height, and Tilt Angle Derived from Solar PV module on a Concrete Surface Measured Parameters

Parameters	Optimal values
Module efficiency (η)	0.22
Module Area (A)	1.998
Front side irradiance (G_{front})	884
Module Bifaciality (δ)	0.80
Surface albedo reflectance (α)	0.961
Maximum theoretical rear-side exposure to ground-reflected irradiance (F_{max})	0.500
Module Mounting Height (h)	1.26
Tilt angle (θ)	10.84
Characteristic height where 63% of F_{max} is reached (H_0)	0.32
Module Power temperature coefficient (γ_P)	0.300
STC temperature	25.00
Cell operating temperature (T_{cell})	60.60
Temperature difference between cell and operating temperature (ΔT)	35.60
view factor	0.9663
Power coefficient from output loss due to cell temperature	0.8932
Output power (Pmax)	474.088

Table 4.6 summarizes the optimal parameters derived from the solar PV module performance on a concrete surface using measured data and the predictive model. The module efficiency was maintained at 22%, with a module area of 1.998 m² and a front-side irradiance of 884 W/m². The bifaciality factor was set at 0.80, while the surface albedo reflectance was optimized to a high value of 0.961, maximizing the rear-side irradiance contribution. The optimal mounting height was determined to be 1.26 meters, paired with a tilt angle of 10.84°, enhancing irradiance capture and energy yield. A characteristic height (H_0) of 0.32 m was identified, indicating the height at which 63% of the maximum theoretical rear irradiance exposure is reached. The cell operating temperature was 60.6°C, resulting in a temperature difference (ΔT) of 35.6°C from the standard test conditions (25°C), with a corresponding power temperature coefficient adjustment of 0.8932. The view factor calculated was 0.9663, all combining to produce an optimized maximum power output (P_{max}) of approximately 474.1 W, closely aligning with the targeted module performance.

Table 4.7: Optimization Model Test for Solar PV module on Concrete Surface (Absolute Albedo value)

Parameters	Optimal values
Module efficiency (η)	0.22
Module Area (A)	1.998
Front side irradiance (G_{front})	884
Module Bifaciality (δ)	0.80
Surface albedo reflectance (α)	0.300
Maximum theoretical rear-side exposure to ground-reflected irradiance (F_{max})	0.500
Module Mounting Height (h)	2.00
Tilt angle (θ)	8.81
Characteristic height where 63% of F_{max} is reached (H_0)	0.32
Module Power temperature coefficient (γ_P)	0.300
STC temperature	25.00
Cell operating temperature (T_{cell})	60.60
Temperature difference between cell and operating temperature (ΔT)	35.60
view factor	0.9663
Power coefficient from output loss due to cell temperature	0.8932
Output power (P_{max})	388.387

Table 4.7 presents the results of the optimization model applied to the solar PV module on a concrete surface using an absolute albedo value of 0.300, which aligns with typical measured reflectance for concrete. While keeping the module efficiency at 22% and area at 1.998 m², the model used a front-side irradiance of 884 W/m² and a bifaciality factor of 0.80. The optimization determined a maximum module mounting height of 2.00 meters and a tilt angle of 8.81°, aiming to enhance rear-side irradiance exposure, with a characteristic height (H_0) of 0.32 m. Despite this configuration, the lower albedo limited the rear-side irradiance contribution, resulting in a reduced maximum output power (P_{max}) of 388.4 W. The cell temperature, estimated at 60.6°C, produced a temperature differential (ΔT) of 35.6°C, leading to a temperature-related power loss coefficient of 0.8932. The view factor remained constant at 0.9663, reflecting strong rear-side exposure geometry. Overall, the lower albedo constrained performance, reaffirming the critical role of surface reflectivity in bifacial PV optimization.

4.4.3.2 Testing with Solar PV Module on Grass Surface

The mean measurements from the experiment on the solar PV module on the grass surface from Table 4.4 indicate that irradiance is 957W/m² and cell operating temperature is 72.4°C. When these measurements are used in the optimization model, the optimum outputs are an albedo factor of 0.847, mounting height of 1.09, and tilt angle of 10.31°. The optimum output is 474.174W, slightly higher than the output established by the experiment with concrete surface. Table 4.8 summarizes the results provided by the optimization model.

Table 4.8: Optimum Albedo, Mounting Height, and Tilt Angle Derived from Solar PV Module on a Grass Surface Measured Parameter

Parameters	Optimal values
Module efficiency (η)	0.22
Module Area (A)	1.998
Front side irradiance (G_{front})	957
Module Bifaciality (δ)	0.80
Surface albedo reflectance (α)	0.847
Maximum theoretical rear-side exposure to ground-reflected irradiance (F_{max})	0.500
Module Mounting Height (h)	1.09
Tilt angle (θ)	10.31
Characteristic height where 63% of F_{max} is reached (H_0)	0.32
Module Power temperature coefficient (γ_P)	0.300
STC temperature	25.00
Cell operating temperature (T_{cell})	72.40
Temperature difference between cell and operating temperature (ΔT)	35.60
view factor	0.9663
Power coefficient from output loss due to cell temperature	0.8932
Output power (Pmax)	474.174

As shown in Table 4.8 when the albedo constraint is changed to a constant of 0.195 (albedo coefficient of grass surface), the optimum mounting height is established to be 2m, and the tilt angle is 8.81°. These parameters provide a power yield of 388.763W, which is also slightly higher than that achieved by the solar PV module on concrete surfaces at constant albedo factors. These results are summarized in Table 4.9.

Table 4.9 Optimization Model Test for Solar PV Module on Grass surface (Absolute Albedo value)

Parameters	Optimal values
Module efficiency (η)	0.22
Module Area (A)	1.998
Front side irradiance (G_{front})	957
Module Bifaciality (δ)	0.80
Surface albedo reflectance (α)	0.195
Maximum theoretical rear-side exposure to ground-reflected irradiance (F_{max})	0.500
Module Mounting Height (h)	2.00
Tilt angle (θ)	8.81
Characteristic height where 63% of F_{max} is reached (H_0)	0.32
Module Power temperature coefficient (γ_P)	0.300
STC temperature	25.00
Cell operating temperature (T_{cell})	72.40
Temperature difference between cell and operating temperature (ΔT)	35.60
view factor	0.9663
Power coefficient from output loss due to cell temperature	0.8932
Output power (Pmax)	388.763

Table 4.9 summarizes the optimization model test results for the solar PV module deployed on a grass surface, using an absolute albedo value of 0.195, which reflects typical reflectance for vegetation-covered terrain. With fixed parameters including module efficiency at 22%, area at 1.998 m², and bifaciality at 0.80, the model used a front-side irradiance of 957 W/m²—slightly higher than that on concrete surfaces. The optimization selected a mounting height of 2.00 meters and a tilt angle of 8.81°, maximizing rear-side exposure despite the relatively low albedo. The calculated cell operating temperature of 72.4°C, combined with a temperature differential (ΔT) of 35.6°C, yielded a temperature loss coefficient of 0.8932. Although the rear-side irradiance gain was limited by the lower grass albedo, the model still predicted a respectable power output (P_{max}) of approximately 388.8 W. This outcome emphasizes the importance of mounting height and geometry in offsetting lower surface reflectivity in bifacial PV systems.

4.5 Discussions of Findings

This study sought to investigate the performance of bifacial solar PV modules under varied albedo conditions. Guided by the main objective of optimizing the performance of solar PV systems when powered with bifacial PV modules in varied albedo conditions, this study looked into variations in albedo, mounting height, and tilt angle and how they can help optimize the performance of bifacial PV modules. The study's specific objectives included evaluating the impact of tropical albedo conditions on the performance of bifacial PV modules and analysing the design attributes, such as installation height and tilt angle, and how they can enhance the performance of bifacial PV modules. The other specific objectives included designing an optimization model that can predict and optimize the performance of bifacial solar PV modules and validating the optimization model using empirical data simulations to ascertain its accuracy and effectiveness in predicting the performance of these modules. The following findings were found.

4.5.1 Impact of Albedo Conditions

This study notes that higher albedo conditions contribute to higher energy outputs for bifacial PV modules. This is notable when experimenting with solar PV module on the concrete surface (albedo coefficient of 0.25-0.35) and the grass surface (albedo coefficient of 0.15-0.25). This study noted that the solar PV module mounted on the concrete surface yielded a mean power output of 381W compared to 366W when experimenting on grass surfaces. Additionally, regarding other performance metrics, experiments with concrete surfaces recorded a higher fill factor overall (FF = 0.72) than with grass surfaces (FF = 0.69). The higher fill factor values imply that with a higher albedo coefficient; the solar PV modules efficiently convert sunlight to usable electrical power. Additionally, the optimization model reveals that optimum power output tends to come from higher albedo coefficients. These findings align with the findings of Riedel-Lyngskær et al. (2022), Raina and Sinha (2020), and Sun et al. (2018), who agree that increasing ground reflectivity would boost bifacial gain.

4.5.2 Influence of View Factor

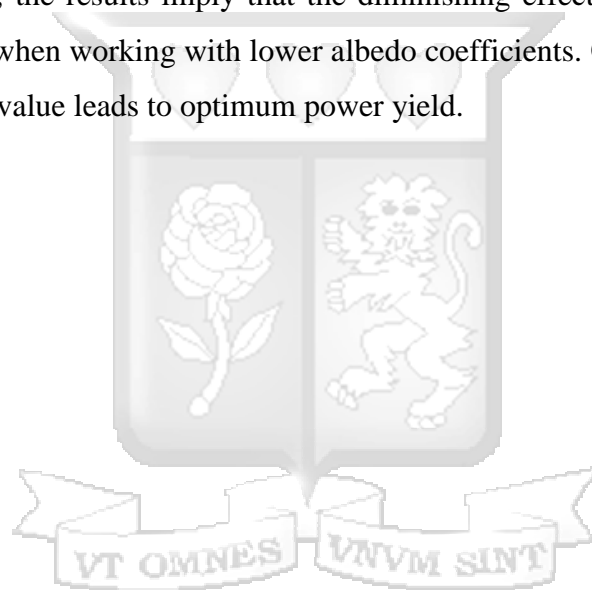
The mounting height and tilt angle determine the view factor. This study's experiment employed a constant tilt angle of 15° while the mounting height was varied. This study finds a consistent increase in energy output with increasing mounting health. In the experiment with the solar PV

module on the concrete surface, when mounting at ground level, the output was 325W; at 0.5 m, the output was 373W; at 1m, the output was 397W; at 1.5m, the output recorded was 428W while at 2m the output was 432W. The results indicate a constant increase in energy yield with increasing mounting height. Similarly, the fill Factor increased from 0.69 at ground level mounting to 0.76 at 2m mounting level. These results implied that the efficiency in energy conversion also increases with mounting height. Similarly, when using the grass surfaces, there was consistency in an increase in energy yield as the mounting height increased. Notably, the energy output measured at ground level was 332W; at the 2m mounting level, the output increased to 389W. These results align with that of Abdeen et al. (2017), who explain that mounting at a higher-level increases air circulation, reducing cell operating temperature. Notably, the cell operating temperature generally decreased with higher mounting height. For the experiment with concrete surface, the cell operating temperature at ground level was 63.3°C, while at 2m mounting height, the cell operating temperature was 58.4°C. Similar trends were observed when experimenting with grass surfaces where the ground level mounting registered a cell operating temperature of 77.2°C while at the 2m mounting level, it was 70.9°C. Higher cell operating temperatures lead to energy loss due to the temperature coefficient. These findings on the effect of mounting height generally agree with the findings of Yusufoglu et al. (2015), who explains that increasing the mounting height would increase the energy yield of bifacial PV modules.

The optimization model also reveals that the view factor depends on the mounting height and the tilt angle. Generally, when the optimization model is set to find the optimum mounting height and tilt angle (view factor), it works out the optimum values to generate the highest possible view factor. According to Table 4.8, the optimal mounting height is 1.26m while the optimum tilt angle is 10.84°; the combination establishes a view factor of 0.9663. According to Liu et al. (2022), while increasing the mounting height correlates with increased energy yield, increasing it beyond a certain point has a diminishing effect. The author explains that higher mounting height contributes to light dispersion and the possibility of self-shading. This explains why the optimization model opts for a lower mounting height when the albedo factor can be optimized. The same trend is notable with results from Table 4.10, in which the optimum mounting height is established to be 1.09m while the optimum tilt angle is set to be 10.31°. The mix establishes a view factor of 0.9663, similar to the results from Table 4.8. Notably, the optimization model settles on a slightly lower tilt angle to attain a similar view factor with a reduced mounting height.

Additionally, this study notes that the optimum tilt angle is far lower than the 15° used in the experiment. According to Abdeen et al. (2017), the optimum tilt angle is attained by balancing self-cleaning capabilities with aligning the PV module to maximum irradiance. At the equator, the closer the tilt angle is to zero, the more irradiance there is, which implies more output. However, a lower tilt angle also means more dust accumulation, which diminishes annual energy yields.

Interestingly, this study also establishes that when the parameters are confined to the absolute albedo coefficient, the optimization model sets the optimum mounting height to 2m, which is also the upper bound limit of the constraints. At the same time, the tilt angle is lowered to 8.84° to attain the same view factor of 0.9663 (Table 4.9). Table 4.11 also indicates a negligible difference in the tilt angle. Overall, the results imply that the diminishing effects of increasing mounting height can be negligible when working with lower albedo coefficients. Overall, the results justify that a higher view factor value leads to optimum power yield.



CHAPTER FIVE CONCLUSION AND RECOMMENDATION

5.1 Conclusion

This study aimed to investigate the performance optimization of bifacial solar photovoltaic (PV) modules under varied albedo conditions in the Kenyan context, addressing a significant gap in the current understanding of how these modules operate in real-world situations. The primary objective was to improve the efficiency of solar PV systems by thoroughly analysing how tropical albedo variations influence the energy production of bifacial modules.

To achieve this, the study outlined several specific objectives, including the evaluation of tropical albedo impacts on bifacial PV performance, the analysis of design attributes like installation height and tilt angle, and the development of an optimization model to predict and enhance energy yield under changing albedo conditions in Kenya. A secondary goal was to validate the optimization model through empirical data collection and simulations.

The data for this study was gathered through an experimental research approach involving systematic measurements of albedo, irradiance, and module cell temperature across ten distinct setups of bifacial PV modules; each mounted at varying heights. The setups were primarily categorized into the first category using concrete surfaces and the second category using grass surfaces. Each surface type had five setups with varying mounting heights (0m, 0.5m, 1m, 1.5m, and 2m). This structured methodology ensured comprehensive data collection and allowed for robust analysis of the performance metrics concerning the environmental conditions.

Key findings revealed that higher albedo values could substantially increase energy output from the backside of bifacial modules. In the study, increasing the albedo coefficient from 0.195 to 0.3 was observed to improve power output from 366W to 381W. Additionally, higher albedo conditions outperform lower albedo conditions in other metrics like cell energy conversion efficiency. These results corroborate theoretical models with empirical evidence. Specifically, the concrete surface with a higher albedo factor consistently performed more than the grass counterpart.

In terms of mounting height, higher mounting heights lead to better energy output. However, there is a diminishing effect on the energy output. Typically, this study finds that between 0m and 1m, there are consistent increases in energy output with an increase in mounting height. After 1m, the increase is negligible and beyond 2m, there are both cost implications and a negative impact on general energy yield. As a key determinant to the view factor, the tilt angle should balance attaining

maximum irradiance and self-cleaning effects. Near the equator region, the optimum tilt angle is between 8° and 15°.

In conclusion, this research contributes valuable insights into the operational efficiency of bifacial solar PV systems in tropical environments, highlighting the importance of understanding albedo dynamics. The findings further illuminate the capabilities of bifacial technology and support the larger goal of advancing sustainable energy practices, offering a pathway for more informed decision-making in solar system design and implementation. The outcomes provide a foundation for future research and practical applications in optimizing solar energy solutions in varied geographical contexts.

5.2 Recommendations

5.2.1 Practical Recommendations

- i. This study recommends the adoption of a bifacial PV module to benefit from additional power output caused by the backside irradiance.
- ii. Other than cost implications, installing bifacial PV modules should involve using the optimum parameters, including enhancing mounting surfaces to those with higher albedo coefficient and using a combination of installation height and tilt angle to improve the view factor.

5.2.2 Recommendations for Future Studies

- i. This study commends that future research should carry out a longitudinal field study to observe the performance of these modules in the Kenyan context over an extended period. Such an approach would allow for a comprehensive understanding of how seasonal and temporal variations in albedo can impact energy output/ this long-term data would also help address the limitations identified in this study, such as the scope of environmental variables and how they influence bifacial module efficiency.
- ii. Future studies should consider integrating advanced simulation techniques combining machine learning algorithms and empirical data to enhance the predictive modelling of bifacial module performance under tropical conditions. By utilizing large datasets and

sophisticated analytical tools, researchers can improve the accuracy of performance predictions under various albedo scenarios. This integration could aid in developing more robust optimization models capable of adapting to real-time environmental changes.

- iii. While this study primarily focused on albedo, installation height, and tilt angles, it is recommended that future studies explore other optimization factors, such as atmospheric conditions, temperature variations, and shading from nearby structures. These factors could play significant roles in determining the overall performance of bifacial PV modules and should be integrated into optimization strategies to maximize energy yield.
- iv. Given the potential benefits of bifacial PV technology outlined in this research, policymakers are encouraged to develop supportive frameworks that promote adopting bifacial systems. This includes establishing standards for installation practices, enabling reflective materials in nearby environments to enhance albedo, and providing financial incentives for adopting advanced solar technologies. Regulatory bodies such as the Energy and Petroleum Regulatory Authority (EPRA) should actively engage with stakeholders in the solar industry to promote these practices.

5.3 Contribution to Existing Knowledge

This study sets the starting point for looking into the implications and applications of bifacial solar PV modules in the Kenyan context. The optimization model's development paved the way for more scholarly research that would build on the current framework to look into the nuanced knowledge base concerned with bifacial PV modules and their applications in Kenya.

References

- Adam, J. (2019). (PDF) *basics of solar PV system*. ResearchGate.
https://www.researchgate.net/publication/336304966_basics_of_solar_PV_system
- Alexander, P. M., Tedesco, M., Fettweis, X., Van De Wal, R. S. W., Smeets, C. J. P. P., & Van Den Broeke, M. R. (2014). Assessing spatiotemporal variability and trends in modeled and measured Greenland Ice Sheet albedo (2000–2013). *The Cryosphere*, 8(6), 2293-2312.
- Amir Asgharzadeh Shishavan. (2019). *Bifacial photovoltaic (PV) system performance modeling utilizing ray tracing*. <https://doi.org/10.17077/etd.wb36-bytp>
- Bojja, S. K., M., K. B., & Murthy, Ch. S. N. (2024). Bifacial Solar PV Systems: A Sustainable Solution for Energy-Intensive Industries. *2024 IEEE 4th International Conference on Sustainable Energy and Future Electric Transportation (SEFET)*, 1–6.
<https://doi.org/10.1109/sefet61574.2024.10717876>
- Borull, M. (2019). *Performance Optimization of Bifacial Module PV Power Plants Based on Simulations and Measurements*. https://reposit.haw-hamburg.de/bitstream/20.500.12738/9131/1/GuariBorullMiriamMA_geschwaerzt.pdf
- Ganesan, K., Winston, D. P., Sugumar, S., & Jegan, S. (2023). Performance analysis of n-type PERT bifacial solar PV module under diverse albedo conditions. *Solar Energy*, 252, 81-90.
- Gevorkov, L., Domínguez-García, J. L., & Romero, L. T. (2022). Review on solar photovoltaic-powered pumping systems. *Energies*, 16(1), 94.

Guerra, N., Guevara, M., Palacios, C., & Crupi, F. (2018). Operation and physics of photovoltaic solar cells: an overview. *I+D Tecnológico*, *14*(2), 84–95.

<https://doi.org/10.33412/idt.v14.2.2077>

Guerrero-Lemus, R. V. T. K. A. K. L. S. R., Vega, R., Kim, T., Kimm, A., & Shephard, L. E. (2016). Bifacial solar photovoltaics—A technology review. *Renewable and sustainable energy reviews*, *60*, 1533-1549.

Han, D., & Kim, S. (2024). Design optimization of large-scale bifacial photovoltaic module frame using deep learning surrogate model. *Scientific Reports*, *14*(1), 14592.

<https://doi.org/10.1038/s41598-024-64594-4>

Hansen, C. W., Stein, J. S., Deline, C., MacAlpine, S., Marion, B., Asgharzadeh, A., & Toor, F. (2016, June). Analysis of irradiance models for bifacial PV modules. In *2016 IEEE 43rd Photovoltaic Specialists Conference (PVSC)* (pp. 0138-0143). IEEE.

International Energy Agency. (2021). *Bifacial Photovoltaic Modules and Systems: Experience and Results from International Research and Pilot Applications 2021 Task 13 Performance, Operation and Reliability of Photovoltaic Systems PVPS*. https://iea-pvps.org/wp-content/uploads/2021/04/IEA-PVPS-T13-14_2021-Bifacial-Photovoltaic-Modules-and-Systems-report.pdf

Janssen, G. J. M., Aken, V., Carr, A., & Mewe, A. A. (2015). *Outdoor Performance of Bifacial Modules by Measurements and Modelling*. *77*, 364–373.

<https://doi.org/10.1016/j.egypro.2015.07.051>

Kılıcı, O., & Koklu, M. (2020). BIFACIAL AND MONOFACIAL PHOTOVOLTAİK MODUL WITH TRACKER SYSTEM ANALYSIS. *Journal of Amasya University the Institute of*

Sciences and Technology, 1(2), 98–112.

<https://dergipark.org.tr/en/pub/jauist/issue/59235/832556>

Kirsh, J. M., CEO of PVEL, Kristan. (2020, October 14). *Five Key Factors In Optimizing Your Bifacial PV Power Plant*. Nextracker. <https://www.nextracker.com/2020/10/five-key-factors-in-optimizing-your-bifacial-power-plants/#:~:text=Albedo%2C%20Module%20Mismatch%20and%20More%3A%20Five%20Key%20Factors>

Kopecek, R., & Libal, J. (2021). Bifacial photovoltaics 2021: status, opportunities and challenges. *Energies*, 14(8), 2076.

Liu, Y., Yao, L., Jiang, H., Lu, N., Qin, J., Liu, T., & Zhou, C. (2022). Spatial estimation of the optimum PV tilt angles in China by incorporating ground with satellite data. *Renewable Energy*, 189, 1249–1258. <https://doi.org/10.1016/j.renene.2022.03.072>

Marion, B. (2021). Measured and satellite-derived albedo data for estimating bifacial photovoltaic system performance. *Solar Energy*, 215, 321–327. <https://doi.org/10.1016/j.solener.2020.12.050>

Osama Ayadi, Mustafa Jamra, Jaber, A., Ahmad, L., & Alnaqep, M. (2021). *An Experimental Comparison of Bifacial and Monofacial PV Modules*. <https://doi.org/10.1109/irec51415.2021.9427864>

Pelaez, A. (2019). *Bifacial Solar Panels System Design, Modeling, and Performance Item Type text; Electronic Dissertation*. https://repository.arizona.edu/bitstream/handle/10150/631283/azu_etd_16881_sip1_m.pdf?sequence=1&isAllowed=y

PVsyst Help Contents. (2024). *PVsyst 7 Help*. Pvsyst.com.

https://www.pvsyst.com/help/index.html?contents_table.htm

Raina, G., & Sinha, S. (2020). A simulation study to evaluate and compare monofacial Vs bifacial PERC PV cells and the effect of Albedo on bifacial performance. *Materials Today: Proceedings*. <https://doi.org/10.1016/j.matpr.2020.08.632>

Riaz, M., Imran, H., & Nauman Zafar Butt. (2020). *Optimization of PV Array Density for Fixed Tilt Bifacial Solar Panels for Efficient Agrivoltaic Systems*.
<https://doi.org/10.1109/pvsc45281.2020.9300670>

Riedel-Lyngskær, N., Ribaconka, M., Pó, M., Thorseth, A., Thorsteinsson, S., Dam-Hansen, C., & Jakobsen, M. L. (2022). The effect of spectral Albedo in bifacial photovoltaic performance. *Solar Energy*, 231, 921–935. <https://doi.org/10.1016/j.solener.2021.12.023>

Russell, T. C. R., Saive, R., Augusto, A., Bowden, S. G., & Atwater, H. A. (2017). The Influence of Spectral Albedo on Bifacial Solar Cells: A Theoretical and Experimental Study. *IEEE Journal of Photovoltaics*, 7(6), 1611–1618.
<https://doi.org/10.1109/jphotov.2017.2756068>

Russell, T. C. R., Saive, R., Augusto, A., Bowden, S. G., & Atwater, H. A. (2017). The Influence of Spectral Albedo on Bifacial Solar Cells: A Theoretical and Experimental Study. *IEEE Journal of Photovoltaics*, 7(6), 1611–1618.
<https://doi.org/10.1109/jphotov.2017.2756068>

Saleem, A., Mehmood, E. K., & Rashid, E. F. (2016, December). The efficiency of solar PV system. In *Proceedings of 2nd International Multi-Disciplinary Conference* (Vol. 19, p. 20).

- Sanjuán, M. Á., Morales, Á., & Zaragoza, A. (2021). Effect of precast concrete pavement albedo on the climate change mitigation in Spain. *Sustainability*, 13(20), 11448.
- Saw, M. H., Khoo, Y. S., Singh, J. P., & Wang, Y. (2017). Enhancing optical performance of bifacial PV modules. *Energy Procedia*, 124, 484–494.
<https://doi.org/10.1016/j.egypro.2017.09.285>
- Shoukry, I., Libal, J., Kopecek, R., Wefringhaus, E., & Werner, J. (2016). Modelling of bifacial gain for stand-alone and in-field installed bifacial PV modules. *Energy Procedia*, 92, 600-608.
- Solar Energy Technologies Office. (2022). *Solar Photovoltaic Cell Basics*. Energy.gov.
<https://www.energy.gov/eere/solar/solar-photovoltaic-cell-basics>
- Sun, X., Khan, M. R., Deline, C., & Alam, M. A. (2018). Optimization and performance of bifacial solar modules: A global perspective. *Applied Energy*, 212, 1601–1610.
<https://doi.org/10.1016/j.apenergy.2017.12.041>
- Urrejola, E., Valencia, F., Fuentealba, E., Deline, C., Pelaez, S. A., Meydbray, J., ... & Stein, J. S. (2020). bifiPV2020 bifacial workshop: a technology overview.
- Yu, B., Song, D., Sun, Z., Liu, K., Zhang, Y., Rong, D., & Liu, L. (2016). A study on electrical performance of N-type bifacial PV modules. *Solar Energy*, 137, 129-133.
- Yusufoglu, U. A., Pletzer, T. M., Koduvelikulathu, L. J., Comparotto, C., Kopecek, R., & Kurz, H. (2015). Analysis of the Annual Performance of Bifacial Modules and Optimization Methods. *IEEE Journal of Photovoltaics*, 5(1), 320–328.
<https://doi.org/10.1109/JPHOTOV.2014.2364406>

Ziar, H., Prudon, B., Lin, F. Y., Roeffen, B., Heijkoop, D., Stark, T., ... & Isabella, O. (2021).

Innovative floating bifacial photovoltaic solutions for inland water areas. *Progress in Photovoltaics: research and applications*, 29(7), 725-743.



Appendices

A- similarity Index



15% Overall Similarity

The combined total of all matches, including overlapping sources, for each database.

Filtered from the Report

- Bibliography
- Quoted Text

Match Groups

- 234** Not Cited or Quoted 13%
Matches with neither in-text citation nor quotation marks
- 36** Missing Quotations 2%
Matches that are still very similar to source material
- 0** Missing Citation 0%
Matches that have quotation marks, but no in-text citation
- 0** Cited and Quoted 0%
Matches with in-text citation present, but no quotation marks

Top Sources

- 9% Internet sources
- 9% Publications
- 11% Submitted works (Student Papers)

Integrity Flags

0 Integrity Flags for Review

No suspicious text manipulations found.

Our system's algorithms look deeply at a document for any inconsistencies that would set it apart from a normal submission. If we notice something strange, we flag it for you to review.

A Flag is not necessarily an indicator of a problem. However, we'd recommend you focus your attention there for further review.



Match Groups

- **234** Not Cited or Quoted 13%
Matches with neither in-text citation nor quotation marks
- **36** Missing Quotations 2%
Matches that are still very similar to source material
- **0** Missing Citation 0%
Matches that have quotation marks, but no in-text citation
- **0** Cited and Quoted 0%
Matches with in-text citation present, but no quotation marks

Top Sources

- 9% Internet sources
- 9% Publications
- 11% Submitted works (Student Papers)

Top Sources

The sources with the highest number of matches within the submission. Overlapping sources will not be displayed.

1	Internet	plus.fluke.com	<1%
2	Internet	www.coursehero.com	<1%
3	Internet	pvpmc.sandia.gov	<1%
4	Internet	www.mdpi.com	<1%
5	Internet	ir.uiowa.edu	<1%
6	Internet	dergipark.org.tr	<1%
7	Internet	www.slideshare.net	<1%
8	Publication	Okoronkwo, Juliette. "Field Characterization and Performance Evaluation of Bifaci...	<1%
9	Internet	www.researchgate.net	<1%
10	Publication	Erin M. Tonita, Christopher E. Valdivia, Annie C. J. Russell, Michael Martinez-Szewc...	<1%

B – Ethical Clearance Approval



2nd December 2024

Mr Okoth Ryan,
ryan.okoth@strathmore.edu

Dear Mr Okoth,

RE: Performance Optimization of Bifacial Solar PV Modules under Varied Albedo Conditions

This is to inform you that SU-ISERC has reviewed and **approved** your above **SU-masters** proposal. Your application reference number is **SU-ISERC2406/24**. The approval period is from **2nd December 2024 to 1st December 2025**.

This approval is subject to compliance with the following requirements:

- i. Only approved documents including (informed consents, study instruments, MTA) will be used.
- ii. All changes including (amendments, deviations, and violations) are submitted for review and approval by SU-ISERC.
- iii. Death and life-threatening problems and serious adverse events or unexpected adverse events whether related or unrelated to the study must be reported to SU-ISERC within 72 hours of notification.
- iv. Any changes anticipated or otherwise that may increase the risks or affected safety or welfare of study participants and others or affect the integrity of the research must be reported to SU-ISERC within 72 hours.
- v. Clearance for the export of biological specimens must be obtained from relevant institutions.
- vi. Submission of a request for renewal of approval at least 60 days prior to the expiry of the approval period. Attach a comprehensive progress report to support the renewal.
- vii. Submission of an executive summary report within 90 days of completion of the study to SU-ISERC.

Before commencing your study, you will be expected to obtain a research license from National Commission for Science, Technology, and Innovation (NACOSTI) <https://research-portal.nacosti.go.ke/> and obtain other clearances needed.

Yours sincerely,

Mr Ambrose Rachier,
Chairperson; SU-ISERC

D – PVA-1500 PV Analyzer Calibration Certificate



CERTIFICATE OF CALIBRATION

Manufacturer: Fluke **Model #:** SOLSENSOR 300V3
Serial #: 6613004 **Description:** Wireless PV Reference Sensor

As Received condition:			
As Shipped condition:	Pass		
Issue date:	2024-08-21		
Calibration date:	2024-08-21	Due date:	2026-08-21

CALIBRATION

Procedure: FPC4504.0004

This calibration is traceable to the International System of Units (SI) through recognized national metrology institutes (NIST, PTB, NPL, NIM, NRC, etc.), radiometric techniques, or natural physical constants. The Quality Management System is certified and is in conformance with ISO 9001. This certificate applies to only the item identified and shall not be reproduced except in full, without the specific written approval by Fluke Corporation. If measurement uncertainties are provided on the certificate of calibration, they are calculated in accordance with the method described in the ISO Guide to the Expression of Uncertainty in Measurement (GUM). The reported expanded uncertainty of measurement is stated as the combined standard uncertainty of measurement multiplied by the coverage factor k such that the coverage probability corresponds to approximately 95% and k=2.

VERIFICATION

Verification Equipment Used

- 20936 Mitutoyo 950-317 Digital Protractor S/N: 23100282 Cal: 2024-03-26 Due: 2025-03-26
- 21044 Newport 91150V-CELL Reference Solar Cell S/N: RQN177186 Cal: 2024-07-18 Due: 2025-07-18
- 20889 Fluke 724 Temperature Calibrator S/N: 64541387MV Cal: 2024-02-29 Due: 2025-02-28
- 20888 Fluke 724 Temperature Calibrator S/N: 64541386MV Cal: 2024-02-29 Due: 2025-02-28

Verification Results

	Nominal Value	Reference Value	Measurement Result	2 Year Specification	Max. Permissible Error	Status
Tilt	20°	19.9°	19.63°	±2°	±1.5°	Pass
Temperature (T1)	50°C	50°C	49.68°C	±2°C	±2°C	Pass
Temperature (T2)	50°C	50°C	49.70°C	±2°C	±2°C	Pass
Irradiance with 0° AOI	700 W/m ²	665.75 W/m ²	666.91 W/m ²	±2%	±1.5%	Pass



Fluke Corporation

PO Box 9090 Everett WA 98206-9090 USA

Telephone
425.347.6100

Facsimile
425.446.5116

Internet
www.fluke.com